NASA TECHNICAL NOTE

NASA TN D-4724

FREE-FLIGHT AND WIND-TUNNEL STUDIES OF DEPLOYMENT OF A DYNAMICALLY AND ELASTICALLY SCALED INFLATABLE PARAWING MODEL

by Alice T. Ferris and H. Neale Kelly

Langley Research Center
Langley Station, Hampton, Va.

NATIONAL AERONAUTICS AND SPACE ADMINISTRATION • WASHINGTON, D. C. • SEPTEMBER 1968

FREE-FLIGHT AND WIND-TUNNEL STUDIES OF DEPLOYMENT OF A DYNAMICALLY AND ELASTICALLY SCALED INFLATABLE PARAWING MODEL

By Alice T. Ferris and H. Neale Kelly

Langley Research Center
Langley Station, Hampton, Va.

NATIONAL AERONAUTICS AND SPACE ADMINISTRATION

For sale by the Clearinghouse for Federal Scientific and Technical Information
Springfield, Virginia 22151 – CFSTI price $3.00

FREE-FLIGHT AND WIND-TUNNEL STUDIES OF DEPLOYMENT OF A DYNAMICALLY AND ELASTICALLY SCALED INFLATABLE PARAWING MODEL

By Alice T. Ferris and H. Neale Kelly
Langley Research Center

SUMMARY

The deployment characteristics of a 1/8-size dynamically and elastically scaled model of an inflatable parawing suitable for the recovery of an Apollo-type spacecraft were investigated in free flight and in the Langley transonic dynamics tunnel using a model which was mounted to permit limited angular freedom. The deployments were of a passive type; that is, there was no powered reel-in or reel-out of the suspension lines. However, a braking system was used to attenuate the dynamic loads in the suspension lines.

The deployment technique was developed in an initial series of wind-tunnel tests. By utilizing the equipment and technique evolved from the wind-tunnel studies, successful free-flight deployments were accomplished and the transient loads associated with the deployments were measured. These results were compared with the results of subsequent wind-tunnel tests.

The general behavior of the parawing during deployment in the wind tunnel and during free flight was similar and loads measured in the wind tunnel can be used to give a preliminary indication of those that will be encountered in free-flight deployments. Thus, it was concluded that the wind tunnel can serve as a useful tool in the development of a deployment technique for an inflatable parawing.

INTRODUCTION

As the size and complexity of spacecraft have increased the need for recovery methods which provide landing-site selection and flare capability prior to touchdown has become increasingly important. One approach to achieving this capability is to provide the spacecraft with an auxiliary kite-like gliding device which is deployed for the final letdown. Collectively known as parawings, the configurations vary from those with all flexible sails to those with the sails attached to rigid or semirigid frames. Although recently more emphasis has been given to the all-flexible version, early work was directed toward configurations with large diameter, semirigid, inflatable frames. For example, extensive research, such as reported in references 1 to 4, was directed toward obtaining aerodynamic data applicable to the inflatable parawing.

Deployment (that is, making the transition from a packaged to a stable gliding configuration) is a process which is critical to the successful application of a parawing. Studies of the deployment of a rigid frame parawing are reported in reference 5. In the present paper, the results of studies of the deployment of an inflatable parawing are presented. The experimental investigation consisted of both wind-tunnel and free-flight studies and employed dynamically and elastically scaled parawing-spacecraft models. The primary objectives of these studies were: (1) to determine a satisfactory deployment technique, (2) to measure the transient loads associated with deployment, and (3) to determine the applicability of wind-tunnel tests to investigations of this nature. In addition to the primary objectives, much useful information about the fabrication of dynamically and elastically scaled inflatable structures was obtained. These latter results were reported in reference 6. Results of an initial wind-tunnel investigation to develop a suitable deployment technique and test equipment for performing wind-tunnel deployments were reported, in part, in reference 7.

Presented herein are: (1) the results of a series of free-flight deployments in which the dynamic behavior of the parawing was studied and the associated transient loads were measured; (2) the results of additional wind-tunnel studies in which variations of the deployment sequence were investigated using improved test equipment; and (3) for continuity, a summary of the results of the wind-tunnel investigation previously reported in reference 6.

SYMBOLS

C_T	suspension-line tension coefficient, $\frac{\text{Suspension-line tension}}{qS}$
E	modulus of elasticity
EI	flexural rigidity, lb-ft^2 (N-m^2)
g	acceleration of gravity, 32.2 ft/sec^2 (9.8 m/sec^2)
l	characteristic length, ft (m)
m	mass, slugs (kg)
q	free-stream dynamic pressure, lb/ft^2 (N/m^2)
r	radius of spacecraft model, in. (cm)
S	wing planform area included between the center lines of the leading-edge members and the trailing edge of the canopy, 19.5 ft^2 (1.81 m^2) (See fig. 1)

V	free-stream velocity, ft/sec (m/sec)
W/S	wing loading, lb/ft^2 (N/m^2)
W_b	boom material weight, oz/yd^2 (kg/m^2)
W_c	canopy material weight, oz/yd^2 (kg/m^2)
ρ	air density, slugs/ft^3 (kg/m^3)
F_b	break strength of boom material, lb/in. (N/m)
F_c	break strength of canopy material, lb/in. (N/m)
F_s	break strength of suspension line, lb (N)

Subscript:

r	ratio of model to prototype

Designation of suspension lines (See fig. 1):

A	front of keel to front of capsule
B	center of keel to rear of capsule
C_{Left}	leading edge to left of capsule
C_{Right}	leading edge to right of capsule
D	rear of keel to rear of capsule

PROTOTYPE

The full-scale parawing-spacecraft combination design on which the models were based had a selected wing loading of 7 lb/ft^2 (335 N/m^2) and a nominal gross mass of 8800 lb (3992 kg). The parawing, similar to a parawing proposed for Gemini, had a conical canopy and equal-length inflatable structural members. The spacecraft design was dynamically and geometrically similar to the Apollo command module.

MODEL

Scaling

The scaling parameters held constant from the prototype to the model included Froude number V^2/gl, mass ratio $m/\rho l^3$, and the elasticity parameter ql^4/EI. In order to establish the scaling factors of the basic dimensions (length, mass, and time), certain factors were arbitrarily fixed. The length scaling factor of 1/8 was chosen to keep the model size compatible with the wind-tunnel test-section size. This length scaling factor, together with the Froude number, fixed the time scaling factor. The mass scaling factor was determined from the restriction that the prototype should be in steady-state glide at an altitude of 40 000 feet (12 192 m). All other important scaling characteristics were determined by dimensional analysis. Studies using representative full-scale inflatable structural members and the corresponding model members were conducted to determine the degree of similarity achieved. The results of these studies, presented in reference 6, indicated that the degree of similarity achieved was very good. A summary of the scaling criteria for the model design is shown in table I.

Parawing

The geometric layout of the model parawing is shown in figure 1. The inflated structure of the parawing consisted of three equal-length members (keel and leading edges) joined at the apex (nose) and maintained at a fixed sweep angle of 55^o by spreader bars. The keel, leading edges, and spreader bar were integrally connected to form a closed pressurized system. The keel and leading edges were 63.0 inches (160.02 cm) long and had a constant diameter of 4.5 inches (11.43 cm). The inflated structure was fabricated from 2 plies of 1.2 oz/sq yd (0.041 kg/m^2) nylon cloth impregnated with neoprene elastomer to form an 11 oz/sq yd (0.373 kg/m^2) fabric. The resulting fabric correctly simulated the prototype elongation rate at the model design inflation pressure of 7.5 lb/in^2 (5.17×10^4 N/m^2).

The canopy was attached at the outboard tangency point along each leading edge and at the top of the keel. The canopy, which had a flat-pattern sweep angle of 45^o, formed aerodynamic lifting surfaces on either side of the keel that approximated conical segments. The canopy, which was fabricated of a single ply of 1.75 oz/sq yd (0.0593 kg/m^2) neoprene-impregnated nylon fabric (zero porosity), properly simulated the prototype mass characteristics.

The parawing was attached to the spacecraft with five suspension lines of 1/16-inch (0.159-cm) stainless-steel aircraft cable. The forward A, diagonal B, and aft D lines were attached to the keel; the C_{Left} and C_{Right} cables were attached to the left and right leading edges, respectively, as shown in figure 1. The lengths of these suspension lines

were such that in the fully deployed gliding configuration, a separation distance of 41.0 inches (104 cm) was maintained between the reference plane of the parawing and the center of gravity of the spacecraft. The center of gravity of the parawing-spacecraft combination was located 71 percent of the keel length aft of the apex of the wing and 58.6 percent of the keel length below the keel center line.

Spacecraft

A drawing of the 1/8-size dynamically scaled spacecraft model is presented in figure 2. The scaled spacecraft weight was 64.4 pounds (29.2 kg) with the center of gravity located 0.81 inch (2.1 cm) forward of the geometrical center line and 5.76 inches (14.6 cm) above the lowest point of the base.

Also shown in figure 2 are the points at which the five suspension lines pass through brass fairleads to storage reels located in the interior of the model. Each reel was equipped with a payout control system to attenuate transient loads. In the initial tests, frictional drag was used as a braking force but proved to be difficult to preset and did not attenuate adequately the loads imposed at the end of suspension-line payout. The hydraulically regulated payout system, shown in figure 3, was developed for the subsequent free-flight and later wind-tunnel tests. The primary features of this system are: (1) braking force highly dependent upon payout rate (viscosity effects) and (2) a cushioning or slowing action as the end of suspension-line payout approaches. As shown in figure 3, the payout system also included instrumentation to indicate suspension-line tension and payout.

In addition to the payout systems, the spacecraft provided housing for a compressed air inflation bottle and pyrotechnic deployment sequence initiators.

Wind-Tunnel-Model Internal Arrangement

As previously mentioned, the wind-tunnel studies were conducted in two parts. In both studies the spacecraft was gimbal mounted on a horizontal bar that spanned the test section as shown in figure 4; however, there were differences in the gimbal-attachment apparatus. For the initial wind-tunnel studies the gimbal attachment consisted of a large, self-alining ball bearing, located at the spacecraft center of gravity. This gimbal arrangement allowed the spacecraft 100° angular freedom in pitch and approximately $\pm 10^{\circ}$ angular freedom in both roll and yaw. An improved gimbal arrangement which was used in the second series of wind-tunnel tests is shown in figure 5. The improved gimbal produced considerably less friction than the original gimbal and provided approximately $\pm 15^{\circ}$ angular freedom in roll and yaw and a full 360° angular freedom in pitch. The angular position of the spacecraft was measured through the use of potentiometers equipped with pinion gears that were mated with appropriately attached racks as shown in figure 5.

A photograph of the wind-tunnel-model spacecraft with side panels removed is shown in figure 6. The photograph shows the cutout for the wind-tunnel mounting bar and the hydraulic payout control systems. Note that the payout systems were canted to aline the load balance with the fairleads so that the cable loads were normal to the axis of the balance. Also shown in the figure are the weights added to the model to obtain the desired moments of inertia.

Free-Flight-Model Internal Arrangement

The free-flight spacecraft housed the same hydraulically regulated payout systems as the wind-tunnel model. In addition, the free-flight spacecraft contained three accelerometers, an onboard oscillograph recorder, a radio receiver, and several battery packs. Because of the placement of the onboard oscillograph recorder, it was impossible to locate the accelerometers on the center of gravity of the model. The longitudinal, normal, and transverse accelerometers were located approximately 5.5 inches (14.0 cm), 7.0 inches (17.8 cm), and 8.5 inches (21.6 cm), respectively, aft of the center of gravity of the model in the plane of symmetry. The longitudinal and transverse accelerometers were approximately 1.6 inches (4.1 cm) below the center of gravity and the normal accelerometer was approximately 1.4 inches (3.6 cm) below the center of gravity. A photograph of the free-flight-model spacecraft with panels removed showing the internal arrangement of some of the equipment is presented in figure 7.

Because of the mass of the equipment and instrumentation on board, only a small amount of weight was allowable for ballasting the model. The allowable weight was sufficient to adjust the center of gravity to the desired location but not great enough to obtain the scaled moments of inertia. The moment of inertia in roll was 13.5 percent low, whereas in yaw it was 20.0 percent high. However, the moment of inertia in pitch was only 1.2 percent low. Since pitch is considered to be the most critical motion during deployment, it was felt that these moments of inertia were acceptable.

The free-flight model was also equipped with an emergency parachute recovery system that was packed in the heat shield. The parachute deployment could be initiated by radio command or would deploy automatically if the voltage in the command system dropped below a preset level.

TEST PROCEDURES

Packaging Sequence

Prior to each complete deployment (both wind tunnel and free flight), the parawing was packaged as shown in figure 8. First, the inflatable members of the model were deflated and the canopy was gathered in accordion-like folds (fig. 8(a)), then each leading

edge was placed beneath the keel (fig. 8(b)). The model was then folded along the keel into a W and attached to the capsule at the apex and aft ends of the members with 1/16-inch (0.159-cm) aircraft cable that passed through pyrotechnic cutters (fig. 8(c)). The suspension lines were attached, the inflation hose was connected, and the packaged model was secured with a canvas cover (fig. 8(d)).

Deployment Sequence

The deployments were of the passive type; that is, there was no powered reel-in or reel-out of the suspension lines. The basic deployment sequence was divided into four steps: cover release, inflation, aft release, and apex release. (See fig. 9.) After the cover-release command, the cover was removed by a drogue parachute that was attached to the top of the cover. A second drogue parachute attached to the apex of the parawing was automatically deployed from inside the cover. At the second step, inflation, the model assumed an inverted V configuration as it inflated with the apex and aft ends still attached to the capsule. When the aft ends of the members were released, the leading edges were straight but the keel was buckled in an inverted L shape since the aft (D) cable was not sufficiently long to allow the keel to straighten. The final step was the release of the apex, which was accomplished by a pyrotechnic cutter that also severed the inflation hose. A check valve maintained the inflation pressure after the inflation hose was cut. After apex release, the model rotated into a flying attitude.

TESTS AND FACILITIES

Wind-Tunnel Studies

The wind-tunnel studies were conducted in the Langley transonic dynamics tunnel. High-speed motion-picture cameras located upstream and on each side of the test section were used to record the transient motions of the model. Spacecraft attitude (pitch, roll, and yaw), suspension-line length and load, and an event signal were recorded by two 14-channel oscillograph recorders.

The wind-tunnel deployments were made at atmospheric static pressure and constant dynamic pressures. The design model dynamic pressure for steady-state glide was 3.5 lb/ft^2 (168 N/m^2). Since the terminal dynamic pressure of the spacecraft model plus drogue was approximately 30 lb/ft^2 (1436 N/m^2), the wind-tunnel deployments were made at dynamic pressures of 3.5 lb/ft^2 (168 N/m^2), 7.0 lb/ft^2 (335 N/m^2), and 10.5 lb/ft^2 (503 N/m^2) (one, two, and three times that required for steady-state glide) to simulate three dynamic pressure conditions that would be encountered during a free-flight deployment. The various deployment steps were initiated individually on command by electrically fired pyrotechnic devices.

Free-Flight Studies

The free-flight studies were conducted at a drop site near Houston, Texas. High-speed motion-picture coverage was obtained from both ground cameras and cameras aboard a drop helicopter. Spacecraft accelerations (normal, transverse, and longitudinal), suspension-line length and load, and an event signal were recorded by an onboard 12-channel oscillograph recorder.

For the first two drops, the deployment was initiated within 2 to 3 seconds after model release so that the dynamic pressure would be low. In the last two drops, the model was allowed to free fall to approximately its terminal velocity before deployment was initiated. For the free-flight studies, the various steps of deployment were initiated individually on radio command by electrically fired pyrotechnic devices identical to those used in the wind-tunnel tests.

RESULTS AND DISCUSSION

Deployment Technique

Initial tests.- Although the results of the initial wind-tunnel tests are presented in reference 7, these results are summarized in this section in the interest of continuity. In general, four conclusions useful to the present investigation were obtained from the initial tests: (1) The transient loads associated with deployment decayed rapidly with little or no interaction between steps. This result seems to indicate that deployment studies may be made in steps at constant dynamic pressures. (2) The measured steady-state suspension-line loads agreed well with those predicted by analysis. This argument indicates that the assumed air-load distribution and steady-state stress-analysis procedure used during design were reasonable. (3) It was indicated by the initial tests that for the configuration tested, it was necessary that a small drogue be attached to the apex of the parawing. This drogue served the dual purpose of providing a positive pitching moment to the parawing to insure clean separation after apex release and also to damp transient motions that immediately follow deployment. (4) A more stable configuration resulted after inflation when the aft ends of the leading-edge members were attached to the capsule at points displaced approximately 30° around the periphery on either side of the keel attachment point rather than to a common point.

Reel-out control.- As previously stated under "Models" and in reference 7, considerable difficulty was encountered in the initial wind-tunnel studies in presetting and maintaining adequate reel-out control with the frictional braking systems. The hydraulic systems used in the present investigation adequately attenuated a wide range of loads; however, the excessively slow reel-out rates of the hydraulic systems tended to

aggravate various model instabilities. Slow reel out also prevented rapid transit through troublesome phases of deployment.

Pitch behavior.- Besides cable reel-out rates, the most significant difference between the initial and subsequent tests was the large pitch-under rates and amplitudes of the spacecraft following aft tiedown release that occurred in the second series of wind-tunnel tests. This pitch behavior was attributed to the greater freedom in pitch provided by improvements in the tunnel mounting system. The free-flight tests with complete freedom exhibited pitch characteristics similar to those observed in the later wind-tunnel studies. These pitch rates and amplitudes may be large enough to be undesirable for manned-spacecraft-recovery applications; moreover, the spacecraft pitched under to large negative angles of attack that delayed apex reel-out and inhibited the rotation of the parawing into the glide configuration. A possible remedy for this undesirable behavior is discussed later.

Instability of the L configuration.- In all tests, the parawing exhibited a roll instability in the inverted L configuration assumed by the parawing following aft tiedown release. The high-speed motion pictures indicated that the attachment point of the apex drogue could be a significant factor in initiating this instability. In the initial wind-tunnel tests (reported in ref. 7) and free-flight tests, the drogue line was attached at the foremost point of the apex. From this attachment point the drogue line tended to slip underneath one side of the wing while the wing was in the apex tiedown phase. In several of the initial wind-tunnel tests, such action by the drogue terminated the run.

Although the same drogue behavior was observed in the free-flight tests, the complete freedom of the spacecraft permitted motions that allowed the drogue line to become untangled. In the present wind-tunnel studies, the drogue attachment point was moved to the top side of the keel. From this attachment point the drogue could not readily slip underneath the wing.

Even with the improved drogue-attachment location, the parawing tended to roll before rotating into a flying attitude. Although the exact cause of this instability is not known, it is believed that this tendency to roll was induced by unequal payout of the leading-edge suspension lines produced by small differences in the performance of the payout attenuation systems. This belief is substantiated by the fact that in the free-flight tests the parawing always rolled to the left whereas in the wind-tunnel tests, in which the left and right payout systems had been interchanged, the model always rolled to the right. From the motion pictures obtained during the wind-tunnel tests, it was ascertained that the parawing exhibited greater stability when positive dihedral (leading edges up) existed prior to and after apex release. Therefore, it appears desirable, from a stability standpoint, to allow the leading-edge cables to reel out quickly and at the same rate.

Elimination of the L configuration.- It was indicated in reference 7 that a practical remedy to the roll instability would be to minimize the time lapse between aft and apex release. In view of the pitch-under behavior of the spacecraft following aft release revealed by the later tests, this remedy seems even more attractive. A three-step deployment, in which the L configuration was eliminated by simultaneously releasing the aft and apex tiedowns, was successfully executed in the preliminary tests; however, the transient loads were slightly higher than those obtained in comparable four-step deployments. A simultaneous release and several rapid aft-apex release sequences were attempted in the present series of wind-tunnel deployments. However, in each case, because of the action of the hydraulic load-attenuation system, apex payout was excessively slow; thus the deployment reverted essentially to the four-step sequence.

A second method of eliminating the L configuration, an apex-first release, was also tried in the course of the present wind-tunnel studies. In this deployment the parawing assumed a trailing-edge-forward attitude after apex release which did not appear to be desirable in view of possible damage induced by sail flapping. However, the relatively rapid transition to a flying attitude following aft release, and the stability of the spacecraft throughout the deployment indicates that such a sequence may warrant further study.

Deployment Loads

Time histories.- The time histories of the wind-tunnel deployments are presented in figures 10 to 16 and the free-flight deployments in figures 17 to 20. Both the wind-tunnel and free-flight time histories show the load in pounds and payout in percent of the total length for each of the five suspension lines. The capsule attitude in pitch, roll, and yaw is presented in terms of angular degrees in the wind-tunnel studies, whereas the free-flight deployment time histories indicate the normal, transverse, and longitudinal accelerations of the spacecraft. The time scale is broken to indicate that there were periods wherein no significant events were occurring.

Both the wind-tunnel and free-flight oscillograph recorders were accurate up to a signal frequency of 600 cps. Since the time histories presented are plotted on a greatly reduced time scale, small high-frequency oscillations have been omitted. In all cases, regardless of frequency, the curves presented pass through the maximum transient loads encountered. It may be noted in several cases that the load is indicated by a hatched band. This band represents large oscillating loads (30 cps or higher). (The upper boundary indicates the maximum load and the lower boundary indicates the minimum load.)

The wind-tunnel time histories of runs 1, 3, and 6 (figs. 10, 12, and 15, respectively) indicate large pitch oscillations of the spacecraft prior to inflation. These oscillations were excited by the unstable drogue chute used to pull off the cover. The

tendency of these oscillations to decay after inflation illustrates the stability of the inflated aft and apex tiedown configuration. In addition, the large pitch-under reaction of the spacecraft after apex release (previously discussed under "Deployment Technique") is clearly indicated by the pitch traces in both the wind-tunnel and free-flight time histories.

The payout rate of the suspension lines corresponds well with the simultaneous tension in the cable. In some cases, such as during inflation, the cable appears to pay out slowly with little or no tension in the cable. Since the braking force of the hydraulic control systems is greatly dependent upon velocity of payout, the suspension lines can pay out slowly at very low loads.

Normalizing deployment loads.- A comparison of the wind-tunnel and free-flight time histories indicates similarity with respect to the time occurrence of loads, reel-out of cables, and capsule motions even though the wind-tunnel results represent the infinite mass condition. Since the dynamic pressures were not measured during the free-flight deployments, no direct comparison can be made between the magnitudes of the wind-tunnel and free-flight loads. In an effort to determine the approximate free-flight dynamic pressures, the model was tested in the Langley spin tunnel in each of its various phases of deployment to determine its drag characteristics. (Because of tunnel limitations, the model could not be tested at full design weight; however, since there was little change in the drag coefficient as the model weight approached design condition, it is felt that the drag coefficients obtained are representative.) By using the drag coefficients obtained from the spin-tunnel tests, together with the free-flight oscillograph records and model-release altitudes, the approximate dynamic pressure or q-profiles for the free-flight deployments were calculated. These profiles are presented in figures 21 to 24. Since the model did not fully inflate instantaneously, two q-profiles were determined. In both cases it was assumed that the drag coefficient changed instantaneously. In one case the change was assumed to occur at the beginning of inflation, whereas in the second case the change was assumed to occur when it appeared from the oscillograph records that inflation was complete. Since most of the maximum transient loads occurred when the model was near terminal velocity in either the inverted V or the L configuration, the time at which the drag coefficient was changed had little effect on the indicated dynamic pressure at maximum load.

With these q-profiles, the maximum transient free-flight suspension-line loads were reduced to coefficient form C_T by using the dynamic pressure read from the lower profile, which gave the more conservative load coefficients. The maximum transient loads for the wind-tunnel and free-flight deployments are presented in coefficient form in table II and table III, respectively. These tables also list factors that were felt to affect the load coefficients or load distributions during the deployments.

Effects of deployment method.- It can be shown that in many cases the method of deployment exerted the primary influence on the loads and load distribution. For example, in the third wind-tunnel deployment, as stated in the remarks in table II, an apex-release-first sequence was made and resulted in a noticeably higher load in cable A for that run. The lower loads recorded in run 7 were a result of the model being inverted so that the gravitational loads of the parawing caused the cables to remain taut and thereby prevented development of snap loads.

The free-flight deployment technique was changed only slightly throughout the testing program and was based on the most promising sequence determined in the preliminary wind-tunnel studies, that is, the four step deployment with a minimum time lapse in the L configuration. The first and second deployments were initiated within 2 to 3 seconds after release from the drop helicopter so that the dynamic pressure would be low, whereas the third and fourth deployments were allowed to free fall for some distance to simulate more nearly the prototype reentry dynamic pressure. This change had little effect on the maximum suspension-line loads since the model quickly approached terminal velocity in the inverted V configuration and the maximum suspension-line loads occurred after this phase.

The first and third deployments did not terminate in the fully deployed gliding configuration. Nevertheless, the data from the successful portion of these deployments were presented since the quantity of free-flight data is limited. The second and fourth deployments were considered to be successful.

In each free-flight deployment, the parawing banked to the left following aft release. During the first free-flight deployment, the parawing did not recover from this banked condition. In the second, third, and fourth free-flight deployments when the parawing recovered from the left bank, a snap load was imposed on the previously slack left leading-edge suspension line. This snap load is evident in the free-flight time histories of these deployments (figs. 18, 19, and 20) and explains the higher loads recorded in the left leading-edge cable in each deployment.

Although the second and fourth free-flight deployments were similar and terminated successfully, the suspension-line loads in the fourth deployment were somewhat higher. No explanation can be found for this variation.

Comparison of wind-tunnel and free-flight loads.- The deployment technique was not perfected during the present investigation and, as a result, the data obtained were random even for most similar deployments. In addition, the quantity of data from similar deployments was insufficient to allow the use of statistical methods for prediction. Therefore, in order to provide some insight into the maximum stress condition encountered in each type of test, a comparison was made of the maximum transient load recorded on any individual suspension line throughout the free-flight tests to the

maximum transient load encountered by the same suspension line in the wind-tunnel tests. For this comparison, the first and third wind-tunnel deployments were not included, since the repeated unloading and resultant snap loads upon reloading in the first deployment and the apex-first release deployment sequence in the third deployment were not felt to be representative. The maximum loads were reduced to coefficient form and are presented in the following table:

Cable	Free-flight load coefficient	Wind-tunnel load coefficient
A	0.30	0.32
B	.49	.54
C	.61	.51
D	.69	.61

Note that the loads in the cables to the keel (A, B, and D) compare favorably. However, the leading-edge-cable loads (cable C) were somewhat lower in the wind-tunnel tests. The lower loads were attributed to the restricted freedom of the wind-tunnel spacecraft model in roll. In addition, flow interference from the mounting system may have reduced the effective dynamic pressure on the wing in the wind-tunnel tests. In any event, these comparisons tend to indicate that loads measured in the wind tunnel can be used to give a preliminary indication of those to be encountered in free-flight deployments and that the wind tunnel can be used as an effective tool in the development of a deployment technique for an inflatable parawing.

CONCLUDING REMARKS

In the present investigation, the wind tunnel was used in the development of a passive deployment sequence for an inflatable parawing-spacecraft model. Initial wind-tunnel tests indicated the need for close control of the various phases of the deployment in order to avoid unstable oscillations and to attenuate the dynamic loads. As a result of these studies, the deployment sequences utilized in subsequent free-flight and wind-tunnel deployments incorporated (1) a three-point aft attachment of the inflatable structural members to improve the stability of the configuration during and immediately after inflation, (2) a small drogue parachute attached to the apex of the parawing to insure clean separation after apex release and to damp the transient motions of the wing after deployment, and (3) a system for controlling the reel-out of the suspension lines in order to attenuate the transient loads.

By utilizing the equipment and the deployment technique developed in the wind tunnel, successful free-flight deployments were accomplished and transient loads associated with the deployments were measured. Subsequently, additional wind-tunnel tests were made and variations of the deployment sequence were investigated. Several of these variations appeared attractive for further study.

In the course of the investigation the deployment technique was not perfected sufficiently to eliminate all random motions and loads; consequently, wide variations were found in the results for even the most similar deployments using the same test techniques. Nevertheless, the present investigation indicated that the general behavior of the parawing during deployment in the wind tunnel and in free flight was similar and that the loads measured in the wind tunnel can be used to give a preliminary indication of those encountered in free-flight deployments. It is therefore concluded that the wind tunnel can serve as a useful tool in the development technique for an inflatable parawing.

Langley Research Center,
National Aeronautics and Space Administration,
Langley Station, Hampton, Va., March 19, 1968,
126-14-02-18-23.

REFERENCES

1. Sleeman, William C., Jr.: Low-Speed Investigation of Cable Tension and Aerodynamic Characteristics of a Parawing and Spacecraft Combination. NASA TN D-1937, 1963.

2. Croom, Delwin R.; Naeseth, Rodger L.; and Sleeman, William C., Jr.: Effects of Canopy Shape on Low-Speed Aerodynamic Characteristics of a 55^{o} Swept Parawing With Large-Diameter Leading Edges. NASA TN D-2551, 1964.

3. Naeseth, Rodger L.: An Exploratory Study of a Parawing as a High-Lift Device for Aircraft. NASA TN D-629, 1960.

4. Sleeman, William C., Jr.; and Johnson, Joseph L., Jr.: Parawing Aerodynamics. Astronaut. Aerosp. Eng., vol. 1, no 5, June 1963, pp. 49-55.

5. Burk, Sanger M., Jr.: Free-Flight Investigation of the Deployment, Dynamic Stability, and Control Characteristics of a 1/12-Scale Dynamic Radio-Controlled Model of a Large Booster and Parawing. NASA TN D-1932, 1963.

6. Raff, Bruce W.: Design and Similitude Testing of Dynamically Scaled Paraglider Model. Vol. 16, part one of Advances in Astronautical Sciences, Norman V. Petersen, ed., Western Periodicals Co. (N. Hollywood, Calif.), c.1963, pp. 731-750.

7. Kelly, H. Neale; and McNulty, James F.: Inflatable Parawing Deployment Studies Using a Dynamically and Elastically Scaled Model. Vol. 16, part one of Advances in Astronautical Sciences, Norman V. Petersen, ed., Western Periodicals Co. (N. Hollywood, Calif.), c.1963, pp. 751-758.

TABLE I.- SCALING CRITERIA FOR MODEL DESIGN

Characteristic	Scaling parameter (a)	Scaling factor	Prototype	Model
Length, l	l_r	1/8	42 ft (12.8 m)	5.25 ft (1.60 m)
Density, ρ	ρ_r	4	5.87×10^{-4} slug/ft^3 (0.303 kg/m^3)	2.38×10^{-4} slug/ft^3 (0.123 kg/m^3)
Mass, m	$\rho_r l_r^3$	1/128	17.2 slugs (251.0 kg)	0.16 slug (2.34 kg)
Gravity, g	g_r	1	32.1 ft/sec^2 (9.78 m/sec^2)	32.2 ft/sec^2 (9.81 m/sec^2)
Time, t	$l_r^{1/2}/g_r$	$1/\sqrt{8}$	0.047 sec/cycle	0.016 sec/cycle
Dynamic pressure, q	$g_r m_r/l_r^2$	1/2	7.0 lb/ft^2 (335 N/m^2)	3.5 lb/ft^2 (168 N/m^2)
Wing area, S	l_r^2	1/64	1250 ft^2 (116 m^2)	19.5 ft^2 (1.8 m^2)
Inflation pressure, p	$\rho_r g_r l_r$	1/2	15 psig (1.03×10^5 N/m^2)	7.5 psig (5.17×10^4 N/m^2)
Wing loading, W/S	$m_r g_r l_r^{-2}$	1/2	7.0 lb/ft^2 (335 N/m^2)	3.5 lb/ft^2 (168 N/m^2)
Boom material weight, W_b	$m_r g_r l_r^{-2}$	1/2	36 oz/yd^2 (1.22 kg/m^2)	11 oz/yd^2 (0.373 kg/m^2)
Canopy material weight, W_c	$m_r g_r l_r^{-2}$	1/2	3.5 oz/yd^2 (0.12 kg/m^2)	1.75 oz/yd^2 (0.06 kg/m^2)
Break strength of boom material, F_b	$m_r g_r l_r^{-1}$	1/16	820 lb/in. (143 604 N/m)	85 lb/in. (14 886 N/m)
Break strength of canopy material, F_c	$m_r g_r l_r^{-1}$	1/16	95 lb/in. (16 637 N/m)	50 lb/in. (8756 N/m)
Break strength of suspension line, F_s	$m_r g_r$	1/128	16 300 lb (72 506 N)	480 lb (2136 N)
Modulus of elasticity, E	$\rho_r g_r l_r^2$	1/16	3800 lb/in. (6.65×10^5 N/m)	230 lb/in. (4.03×10^4 N/m)

[a]Subscript r denotes ratio of model to prototype.

TABLE II.- MAXIMUM TRANSIENT LOADS FOR WIND-TUNNEL DEPLOYMENT

Suspension line	Load, lb (N)	C_T	Remarks
	Run 1: q = 3.5 lb/ft^2 (168 N/m^2)		
A	50.3 (223.7)	0.74	Suspension line A payout was excessively slow and caused the parawing to lose lift several times following apex tiedown release. Roll instability following aft tiedown release was minimal.
B	59.0 (262.4)	.86	
C_{Left}	42.8 (190.4)	.62	
C_{Right}	36.1 (160.6)	.53	
D	52.4 (233.1)	.69	
	Run 2: q = 7.0 lb/ft^2 (335 N/m^2)		
A	43.0 (191.3)	0.31	Parawing rolled to right following aft tiedown release. Right spreader bar remained buckled after deployment. No records were obtained for leading-edge suspension-line loads or payout.
B	51.7 (230.0)	.38	
C_{Left}	--- (----)	---	
C_{Right}	--- (----)	---	
D	75.5 (335.8)	.55	
	Run 3: q = 7.0 lb/ft^2 (335 N/m^2)		
A	58.3 (259.3)	0.43	The apex of the parawing was released first. There was a slight fouling of the aft end of the right leading-edge member on the spacecraft following aft tiedown release.
B	52.4 (233.1)	.38	
C_{Left}	59.1 (262.9)	.43	
C_{Right}	41.3 (183.7)	.30	
D	92.9 (413.2)	.68	
	Run 4: q = 7.0 lb/ft^2 (335 N/m^2)		
A	42.2 (187.7)	0.31	The spacecraft was locked at an angle of attack of 90^o until inflation. The parawing rolled to the right following aft tiedown release.
B	59.3 (263.8)	.43	
C_{Left}	51.6 (229.5)	.38	
C_{Right}	56.0 (249.1)	.41	
D	83.6 (371.9)	.61	
	Run 5: q = 7.0 lb/ft^2 (335 N/m^2)		
A	36.6 (162.8)	0.27	The spacecraft was fixed in a glide attitude throughout the deployment. The deployment sequence was begun from the inflated aft and apex tiedown phase. The model rolled to the right and inverted before achieving a flying attitude.
B	69.2 (307.8)	.51	
C_{Left}	40.6 (180.6)	.30	
C_{Right}	69.5 (309.2)	.51	
D	61.4 (273.1)	.45	
	Run 6: q = 10.5 lb/ft^2 (503 N/m^2)		
A	66.5 (295.8)	0.32	The aft and apex tiedowns were released simultaneously; however, deployment reverted to the basic deployment sequence since apex payout was delayed. Parawing rolled to right following aft release.
B	111.1 (494.2)	.54	
C_{Left}	85.7 (381.2)	.42	
C_{Right}	93.9 (417.7)	.46	
D	74.6 (331.8)	.36	
	Run 7: q = 7.0 lb/ft^2 (335 N/m^2)		
A	36.3 (161.5)	0.27	The model was mounted in an inverted position. The inflation hose fouled on the spacecraft and delayed apex release. The roll instability during apex tiedown was minimal.
B	34.6 (153.9)	.25	
C_{Left}	48.3 (214.8)	.35	
C_{Right}	41.0 (182.4)	.30	
D	48.7 (216.6)	.36	

TABLE III.- MAXIMUM TRANSIENT LOADS FOR FREE-FLIGHT DEPLOYMENT

Suspension line	Load, lb (N)	q, lb/ft^2 (N/m^2) (a)	C_T	Remarks
		Drop 1		
A	68.3 (303.9)	11.59 (555)	0.30	The parawing rolled to the left following aft tiedown release and did not recover from the ensuing spin. Check valve in the inflation system also failed.
B	93.3 (415.2)	7.85 (376)	.61	
C_{Left}	94.4 (420.1)	7.85 (376)	.62	
C_{Right}	97.0 (431.7)	7.85 (376)	.63	
D	66.3 (295.0)	11.60 (555)	.29	
		Drop 2		
A	52.0 (231.4)	11.60 (555)	0.23	The apex drogue line went under the wing in the apex tiedown phase. The parawing rolled to the left following aft release; however, the model recovered and achieved a flying attitude. The check valve did not seat properly and caused a gradual loss of inflation pressure.
B	41.3 (183.8)	11.78 (564)	.18	
C_{Left}	138.5 (616.3)	11.60 (555)	.61	
C_{Right}	65.6 (291.9)	7.80 (373)	.43	
D	104.2 (463.7)	7.80 (373)	.69	
		Drop 3		
A	43.4 (193.1)	11.68 (559)	0.19	No motion-picture coverage was obtained of this deployment. The observers noted left roll of the parawing following aft release. Poor visibility prompted the deployment of the emergency parachutes. It appears from the oscillograph records that the model was pulling up into a flying attitude just as the emergency parachutes fired.
B	54.8 (243.9)	11.68 (559)	.24	
C_{Left}	108.6 (483.3)	11.68 (559)	.48	
C_{Right}	99.8 (444.1)	7.90 (378)	.65	
D	82.2 (365.8)	7.90 (378)	.53	
		Drop 4		
A	59.8 (266.1)	10.50 (503)	0.29	The drogue line went under the parawing in the apex tiedown phase. The parawing rolled to the left following aft tiedown release. The model achieved a flying attitude and made several 360^o turns before touching down.
B	99.9 (444.6)	10.50 (503)	.49	
C_{Left}	138.5 (616.3)	11.80 (565)	.60	
C_{Right}	106.6 (474.4)	8.20 (393)	.67	
D	115.8 (515.3)	11.63 (557)	.51	

[a]Dynamic pressure at which the suspension line experienced its maximum transient load.

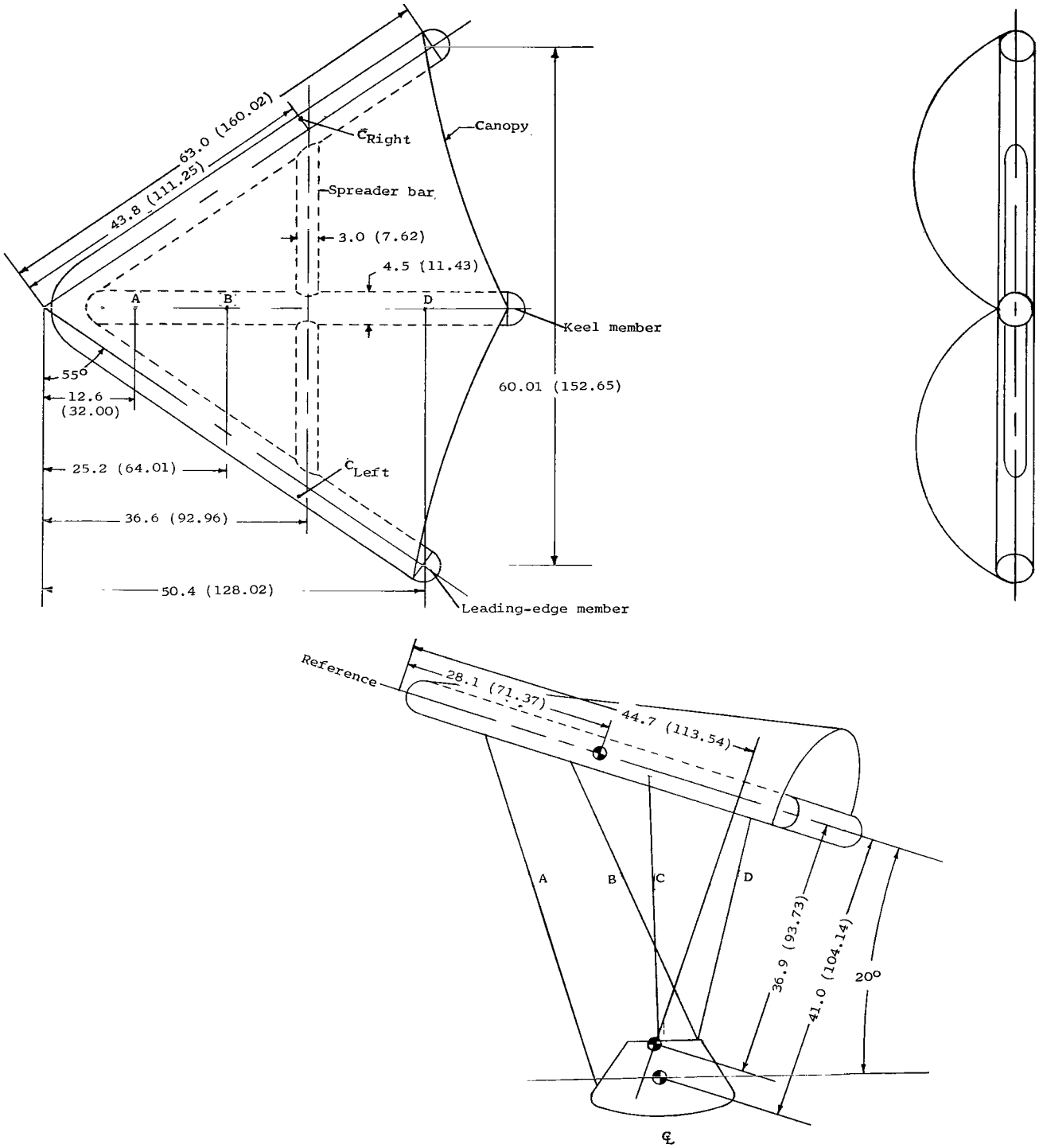

Figure 1.- General arrangement of parawing-spacecraft model configuration. All linear dimensions are in inches (centimeters).

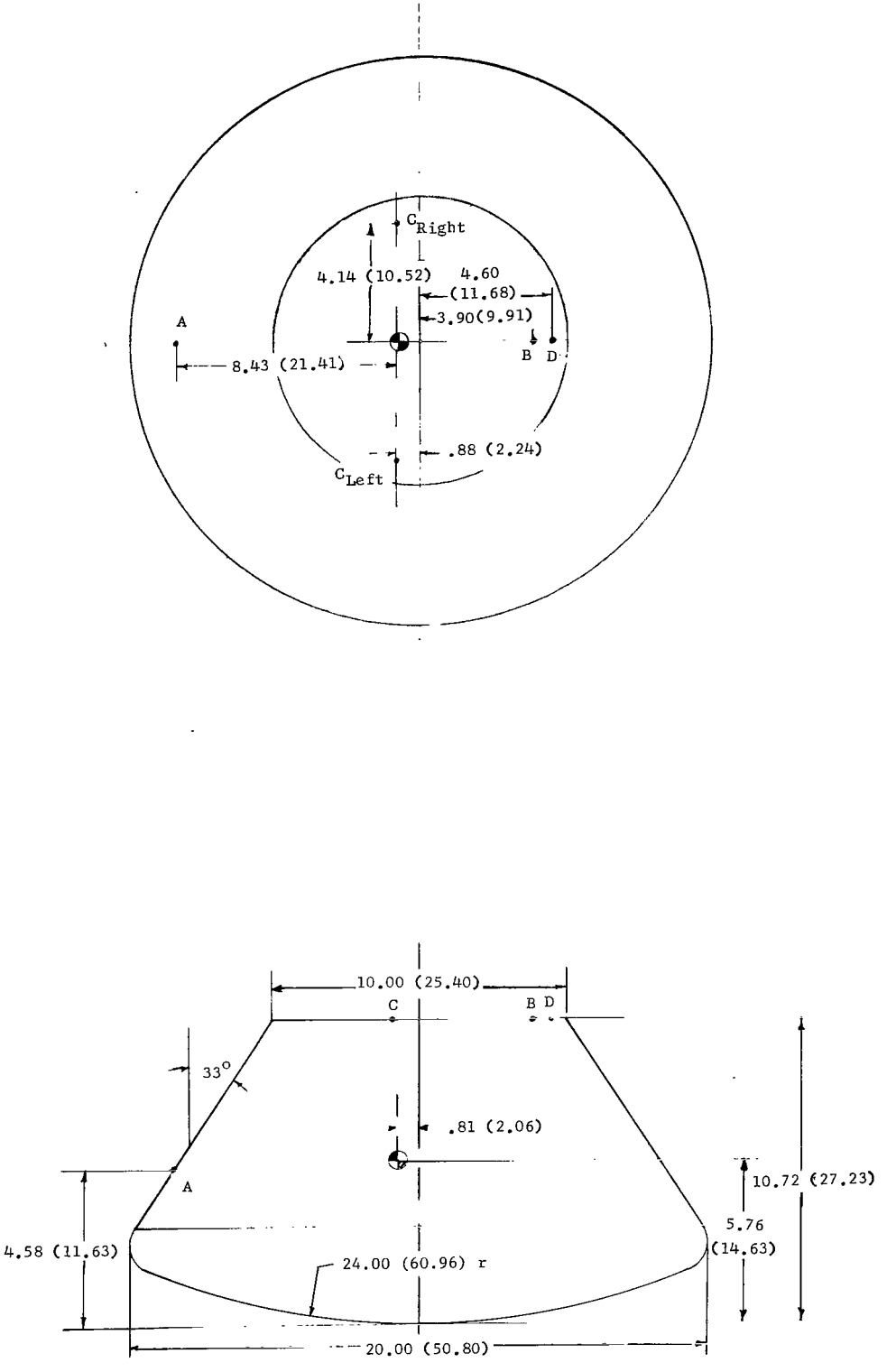

Figure 2.- Geometric layout of spacecraft model. All linear dimensions are in inches (centimeters).

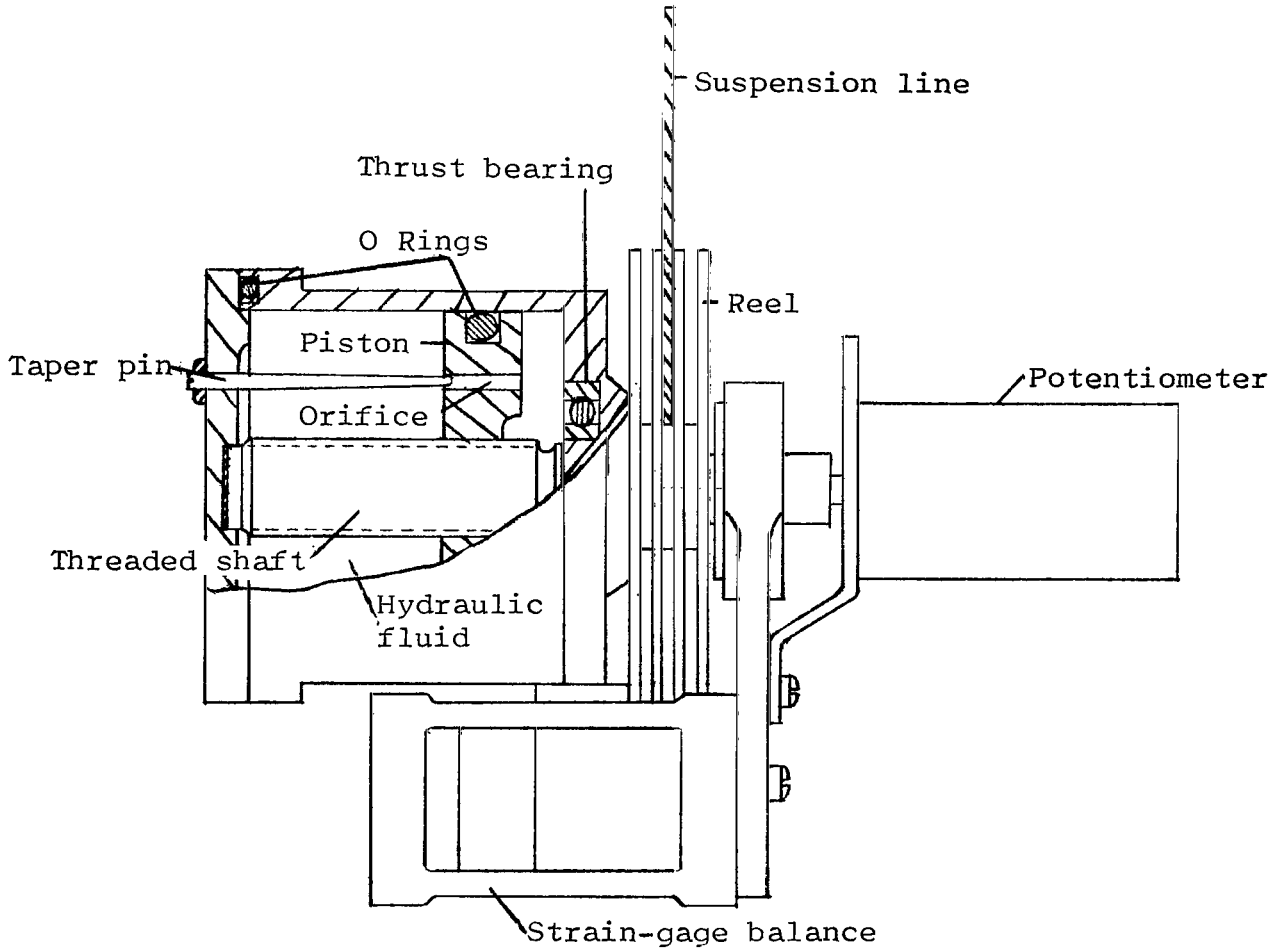

Figure 3.- Hydraulically regulated suspension-line payout system.

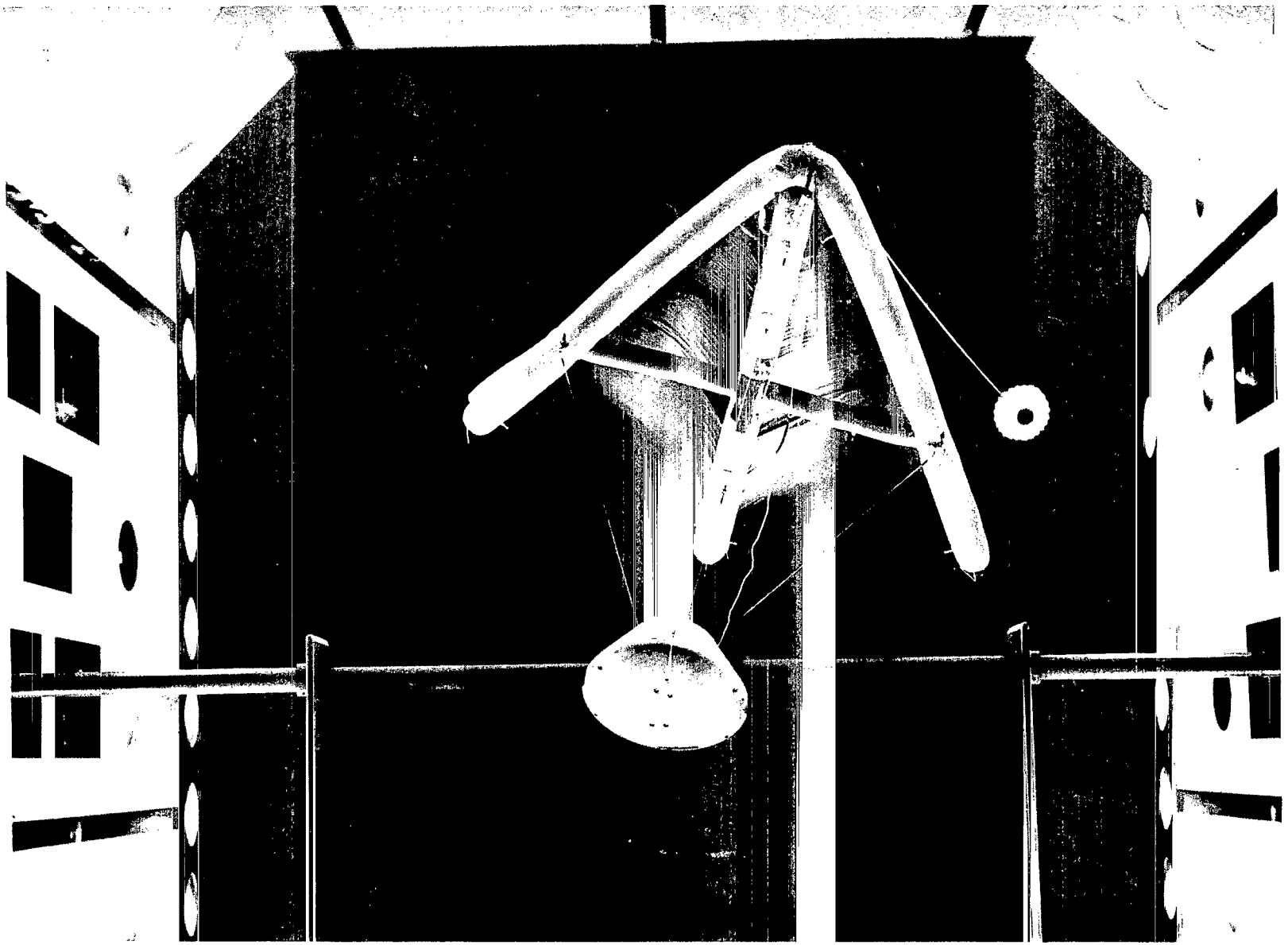

Figure 4.- Fully deployed parawing-spacecraft model mounted in Langley transonic dynamics tunnel.

L-62-8834

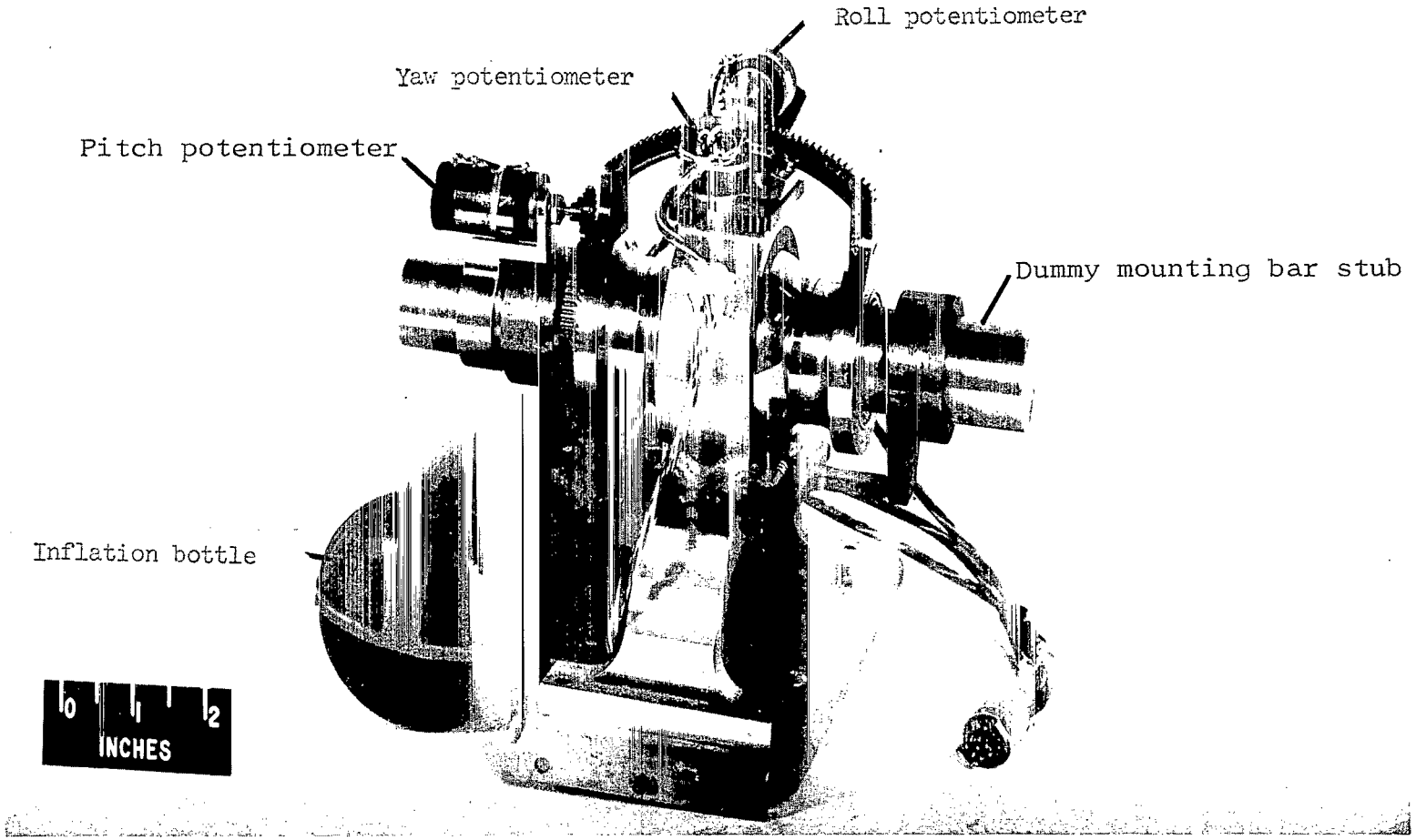

Figure 5.- Gimbal mounting system.

L-65-1449

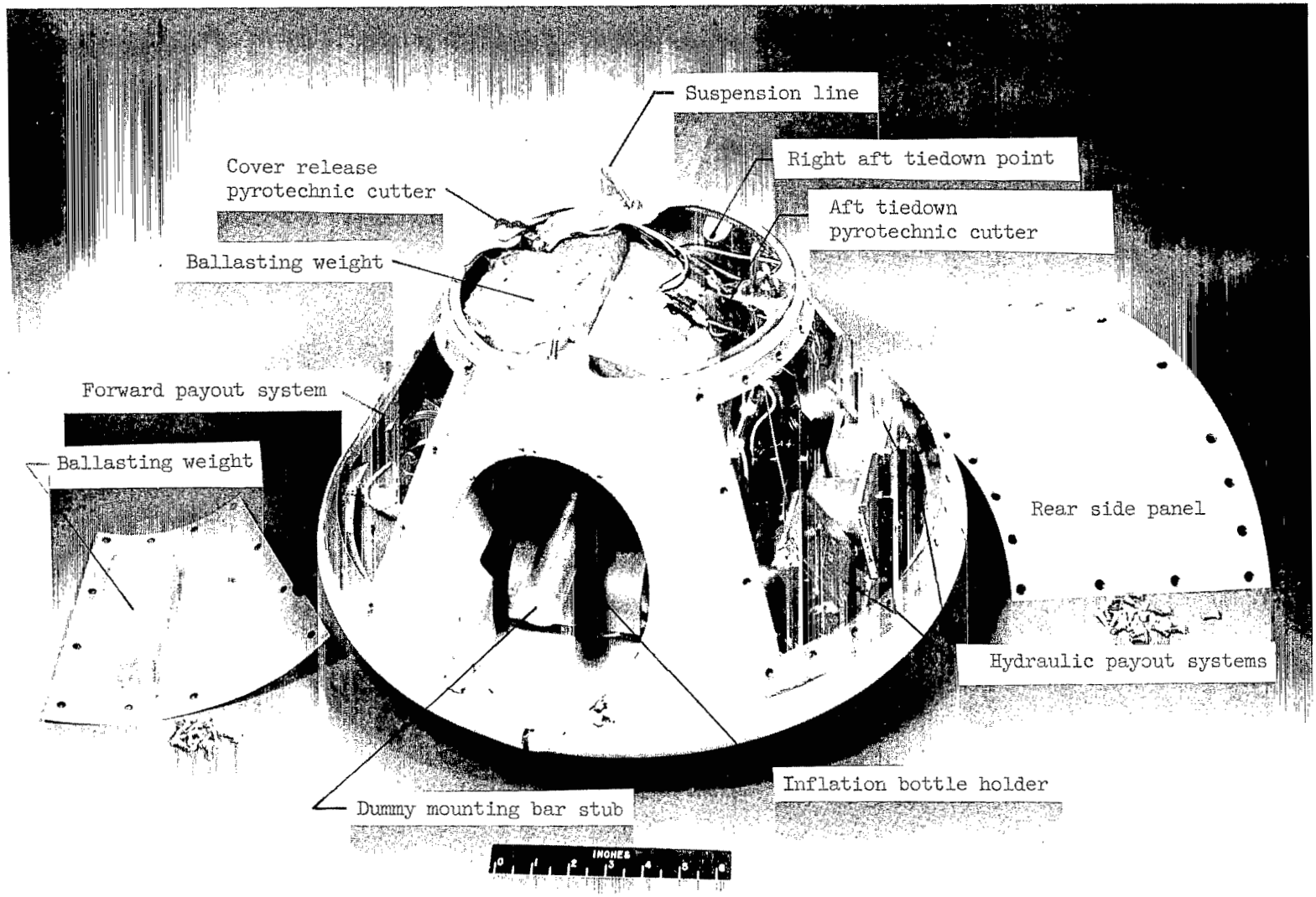

Figure 6.- Wind-tunnel-model spacecraft with side panels removed. L-65-5999

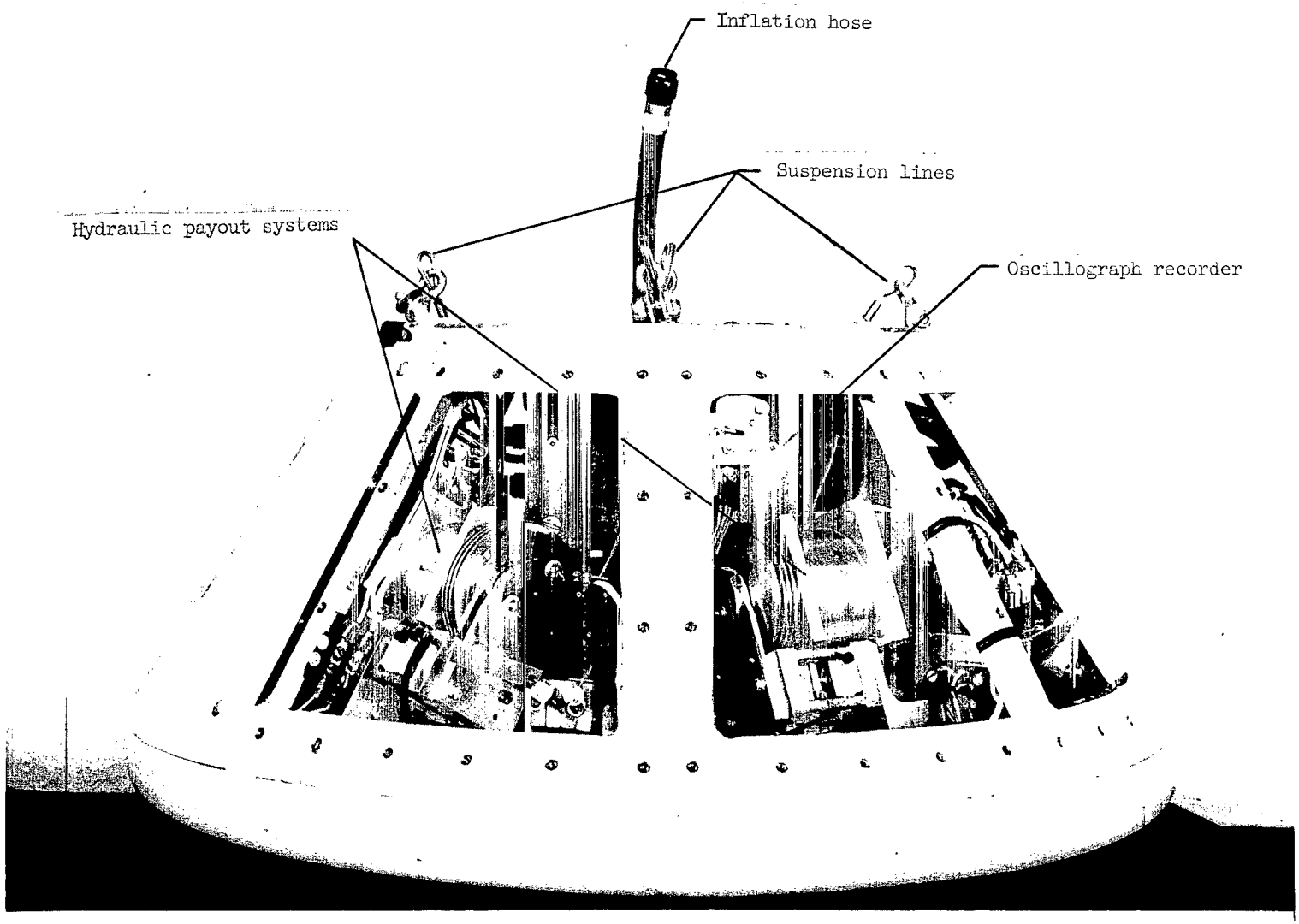

Figure 7.- Rear view of free-flight-model spacecraft with side panels removed. L-63-17460

(a) Deflated model.

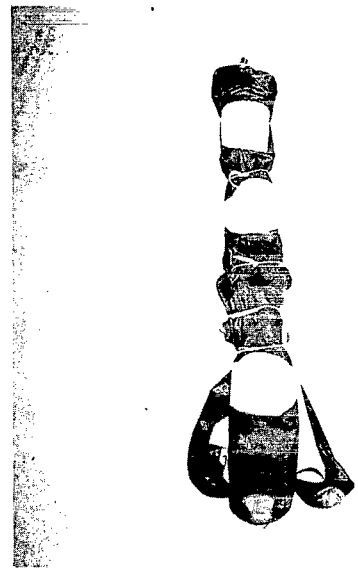

(b) Leading-edge members placed beneath keel.

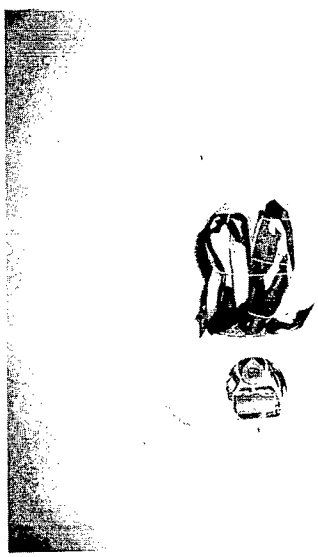

(c) Model in inverted W configuration.

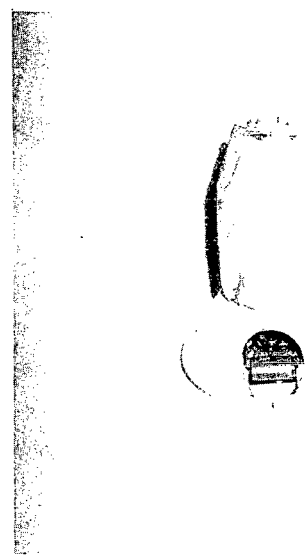

(d) Model secured by canvas cover.

Figure 8.- Packaging sequence. L-68-891

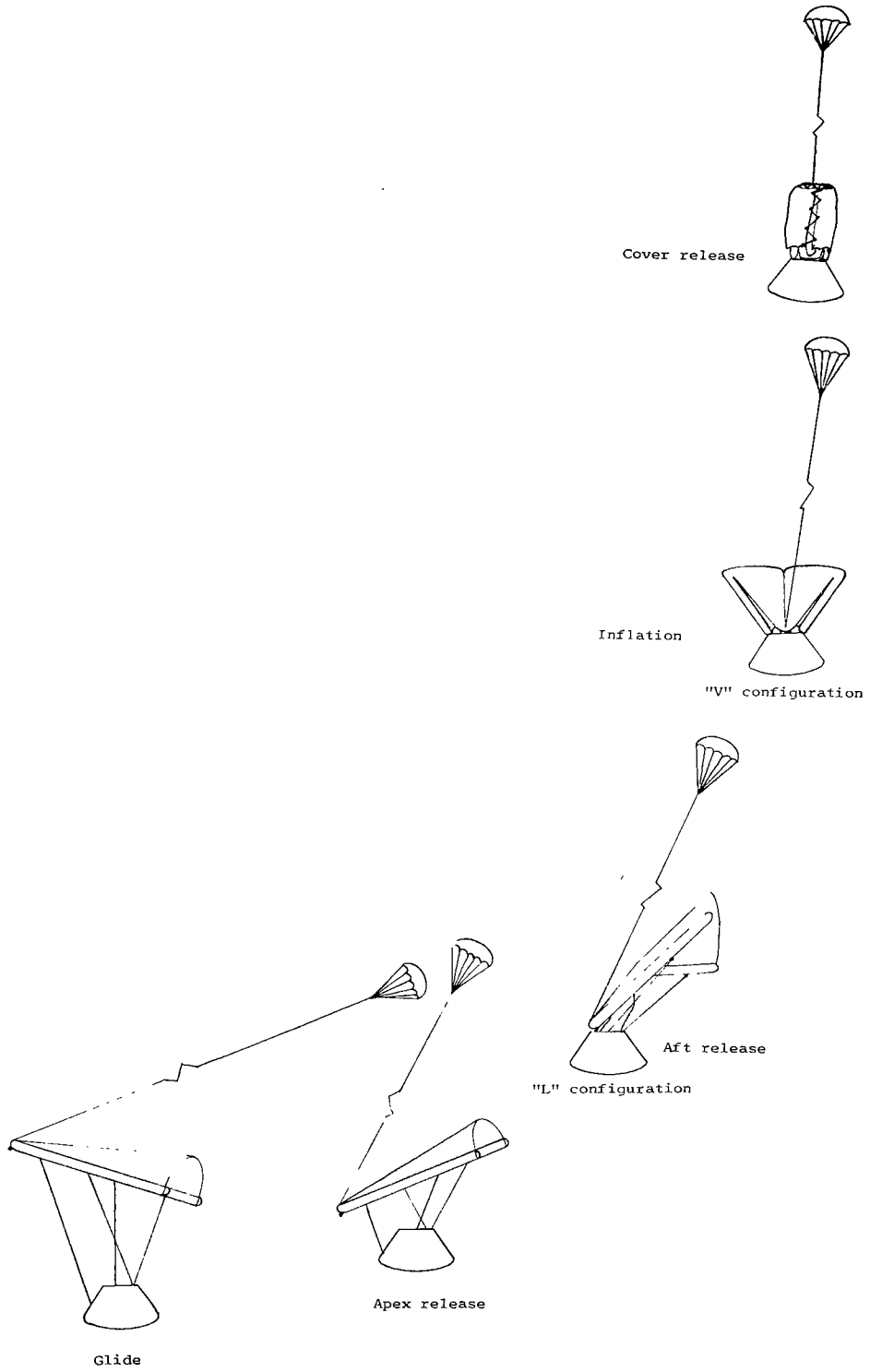

Figure 9.- Deployment sequence.

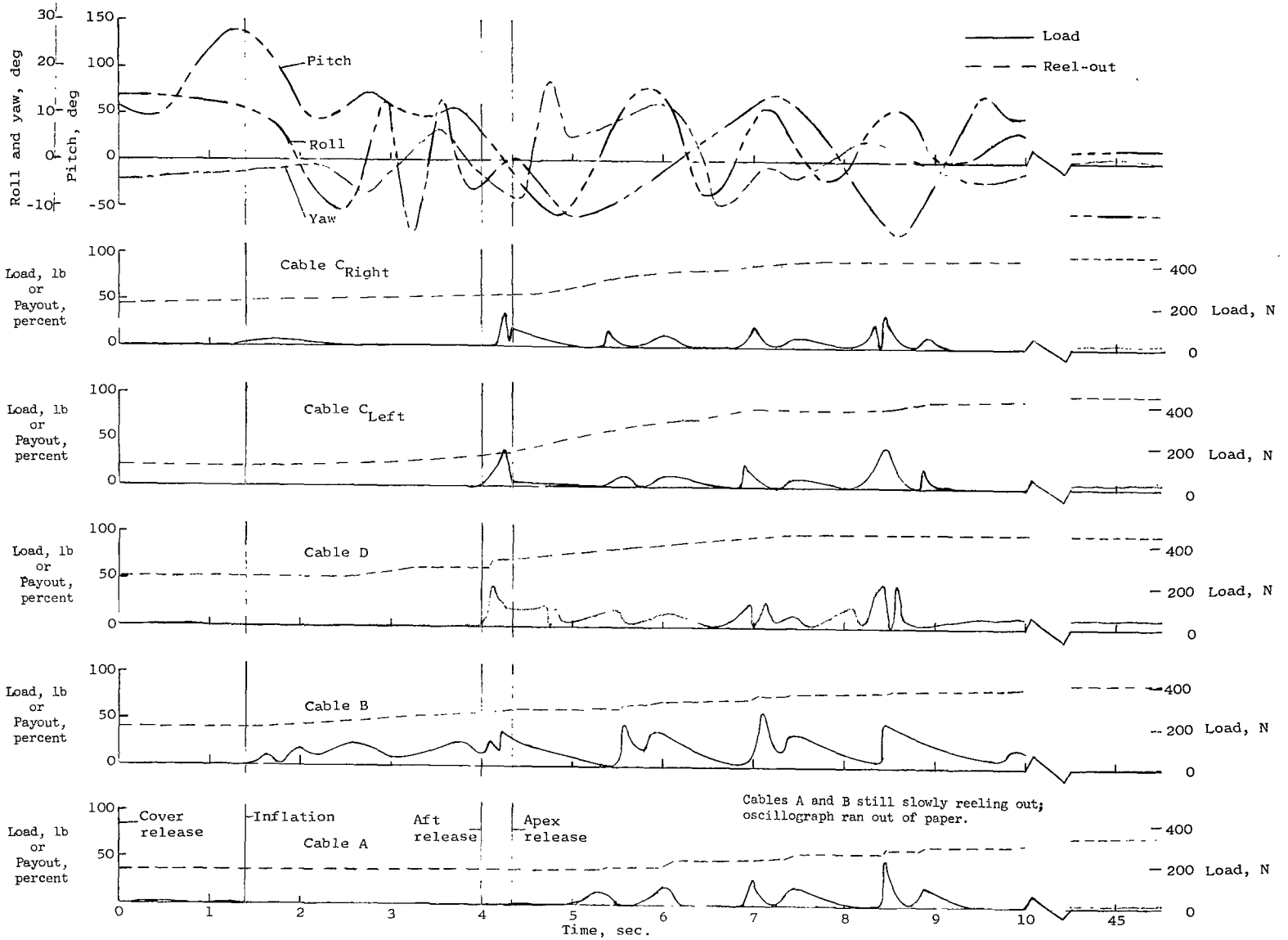

Figure 10.- Time history of first deployment in Langley transonic dynamics tunnel. $q = 3.5$ lb/ft^2 (167 N/m^2).

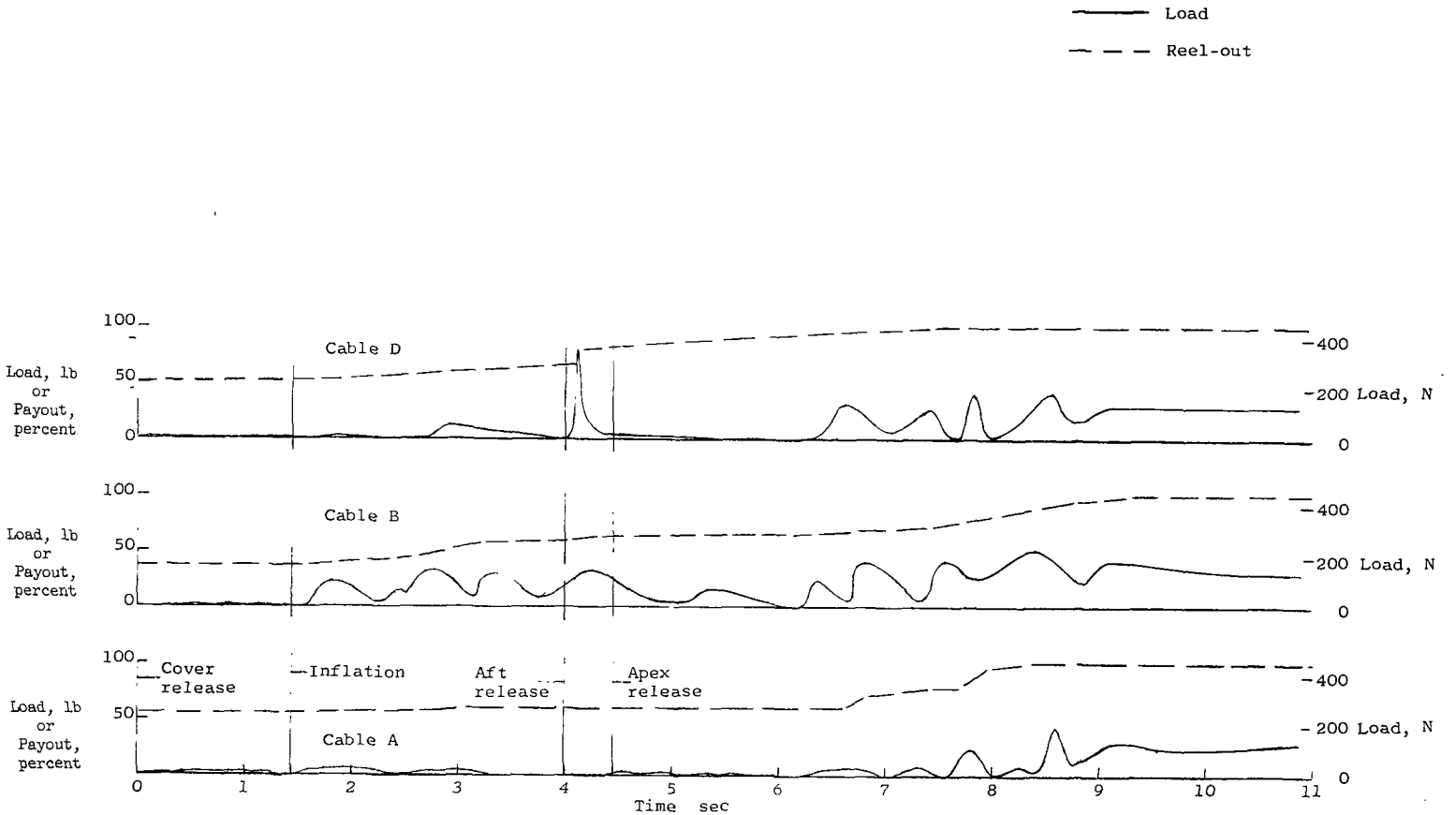

Figure 11.- Time history of second deployment in Langley transonic dynamics tunnel. $q = 7.0\ lb/ft^2$ $(335\ N/m^2)$. No record obtained of cable C_{Left}, cable C_{Right}, pitch, roll, and yaw.

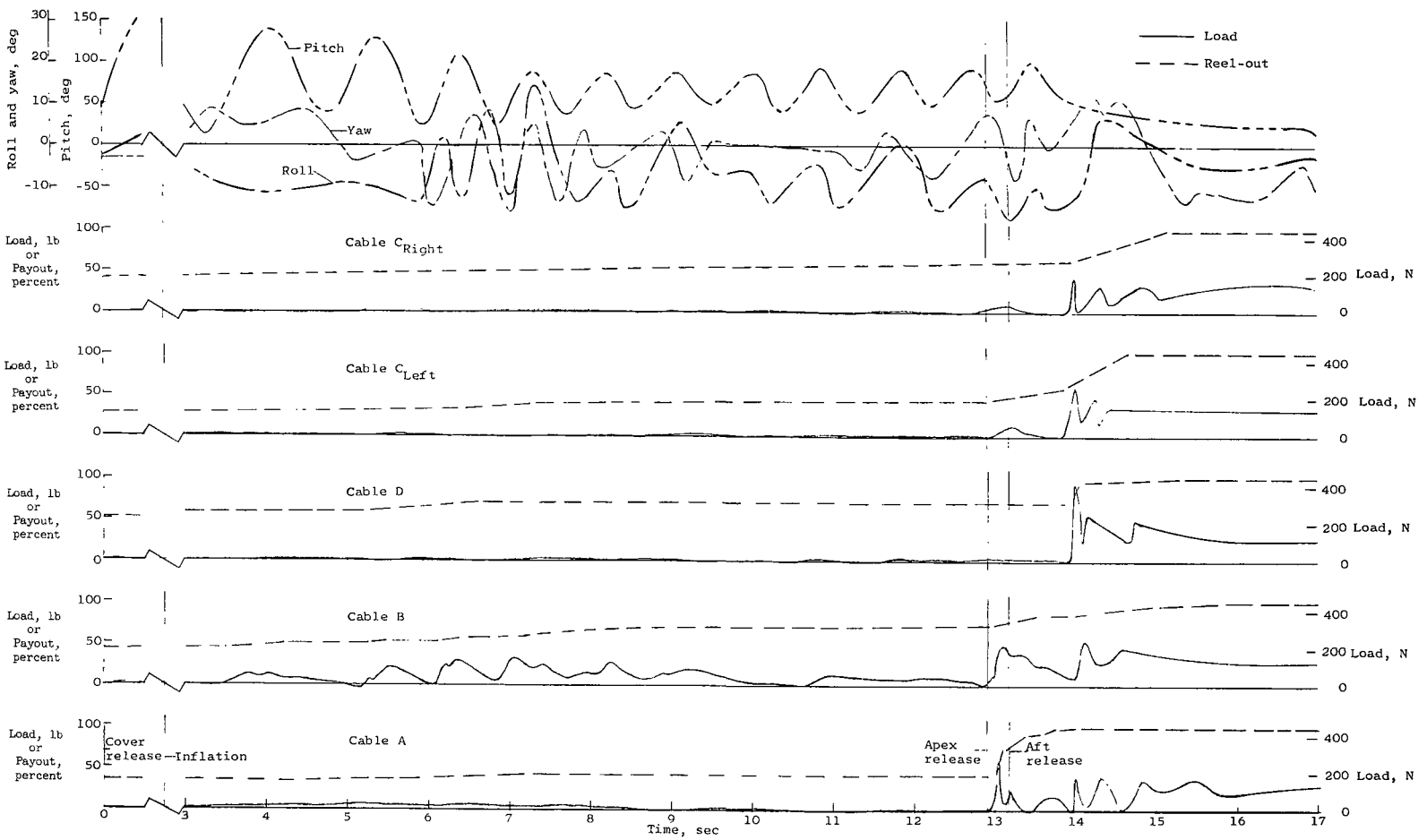

Figure 12.- Time history of third deployment in Langley transonic dynamics tunnel. $q = 7.0$ lb/ft^2 (335 N/m^2). (Apex-release first).

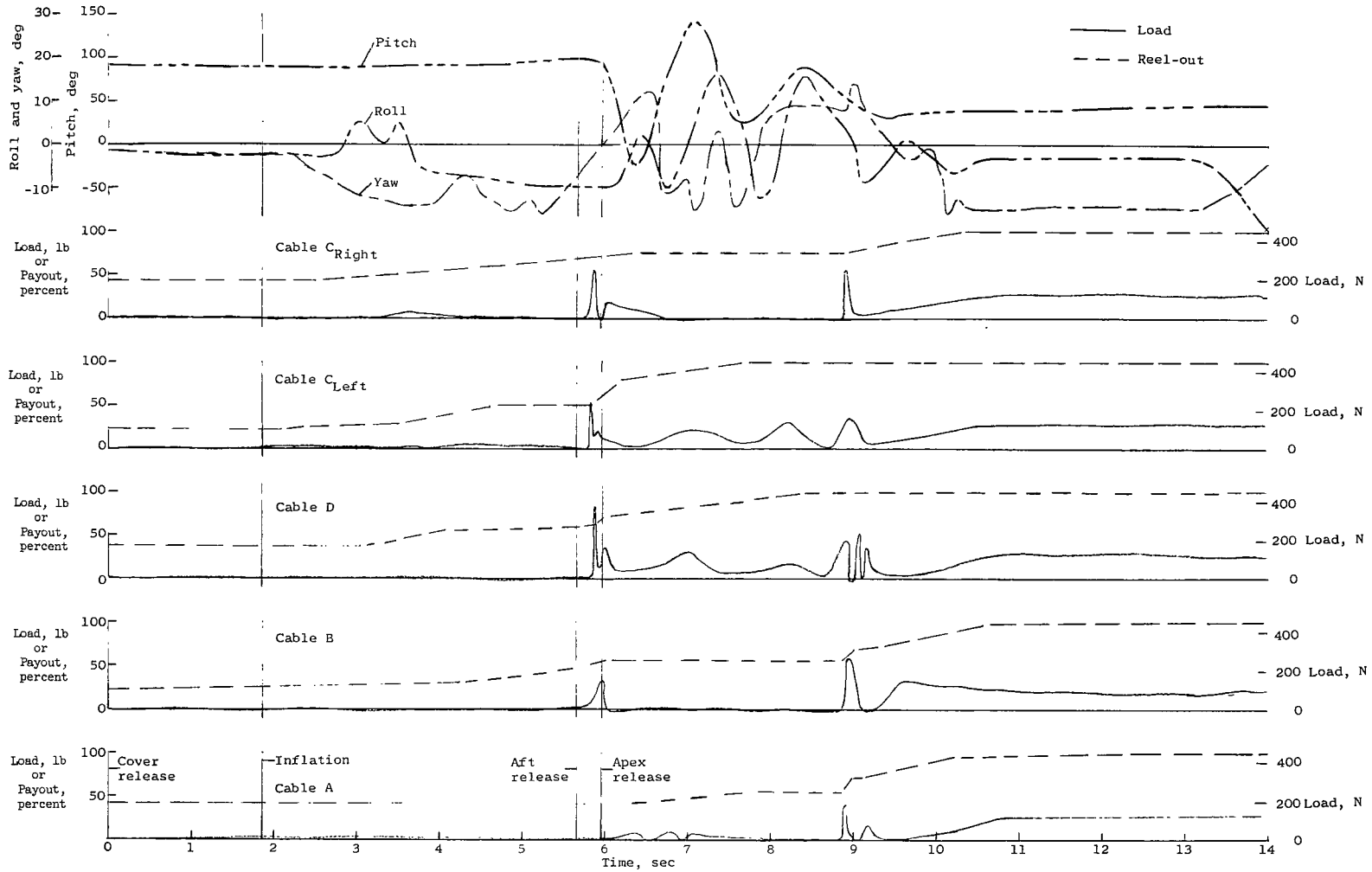

Figure 13.- Time history of fourth deployment in Langley transonic dynamics tunnel. $q = 7.0\ lb/ft^2$ $(335\ N/m^2)$.

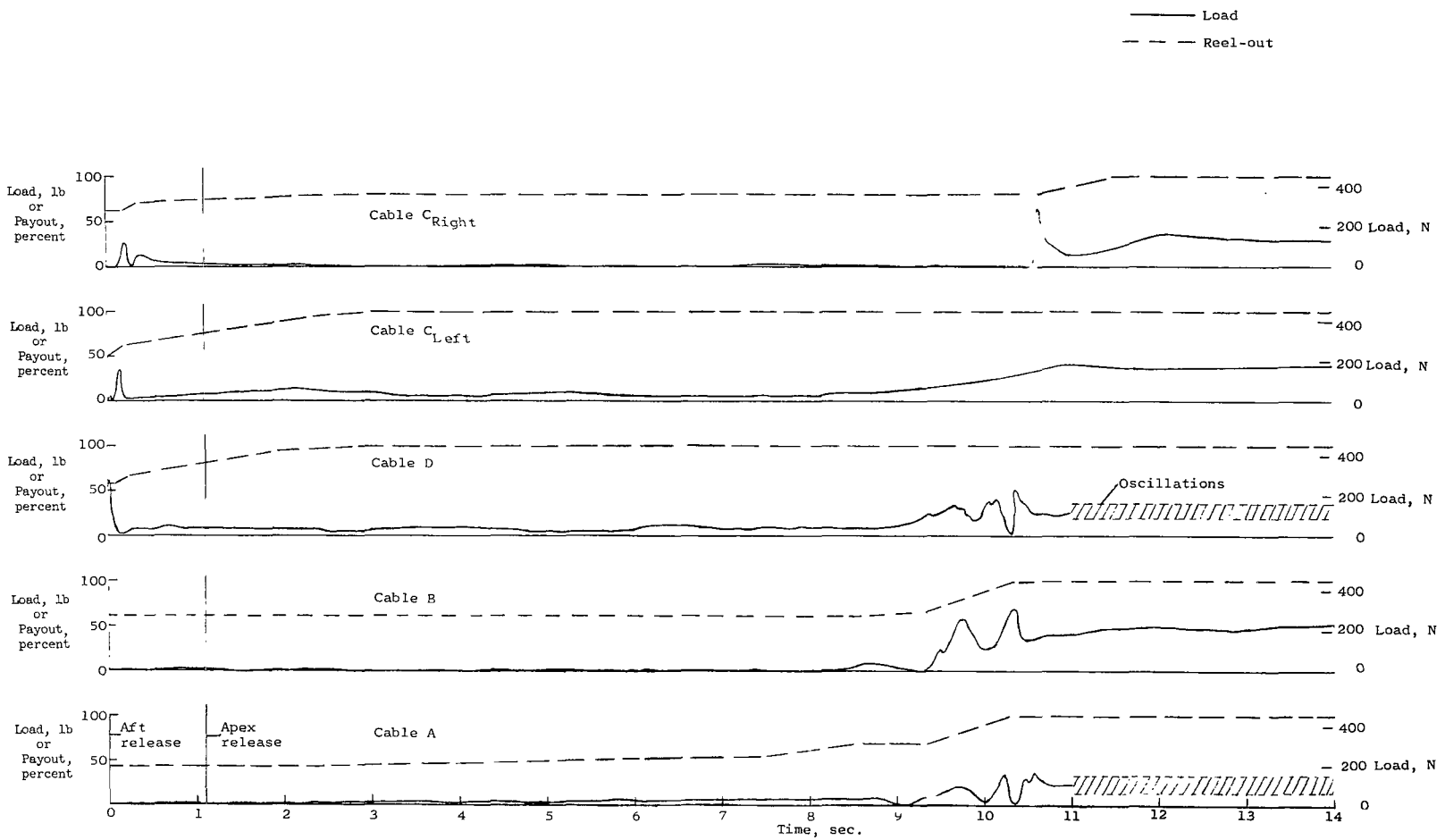

Figure 14.- Time history of fifth deployment in Langley transonic dynamics tunnel. $q = 7.0$ lb/ft^2 (335 N/m^2). Capsule fixed at $\alpha = 20^0$. Deployment begun from inflated apex and aft tiedown configuration.

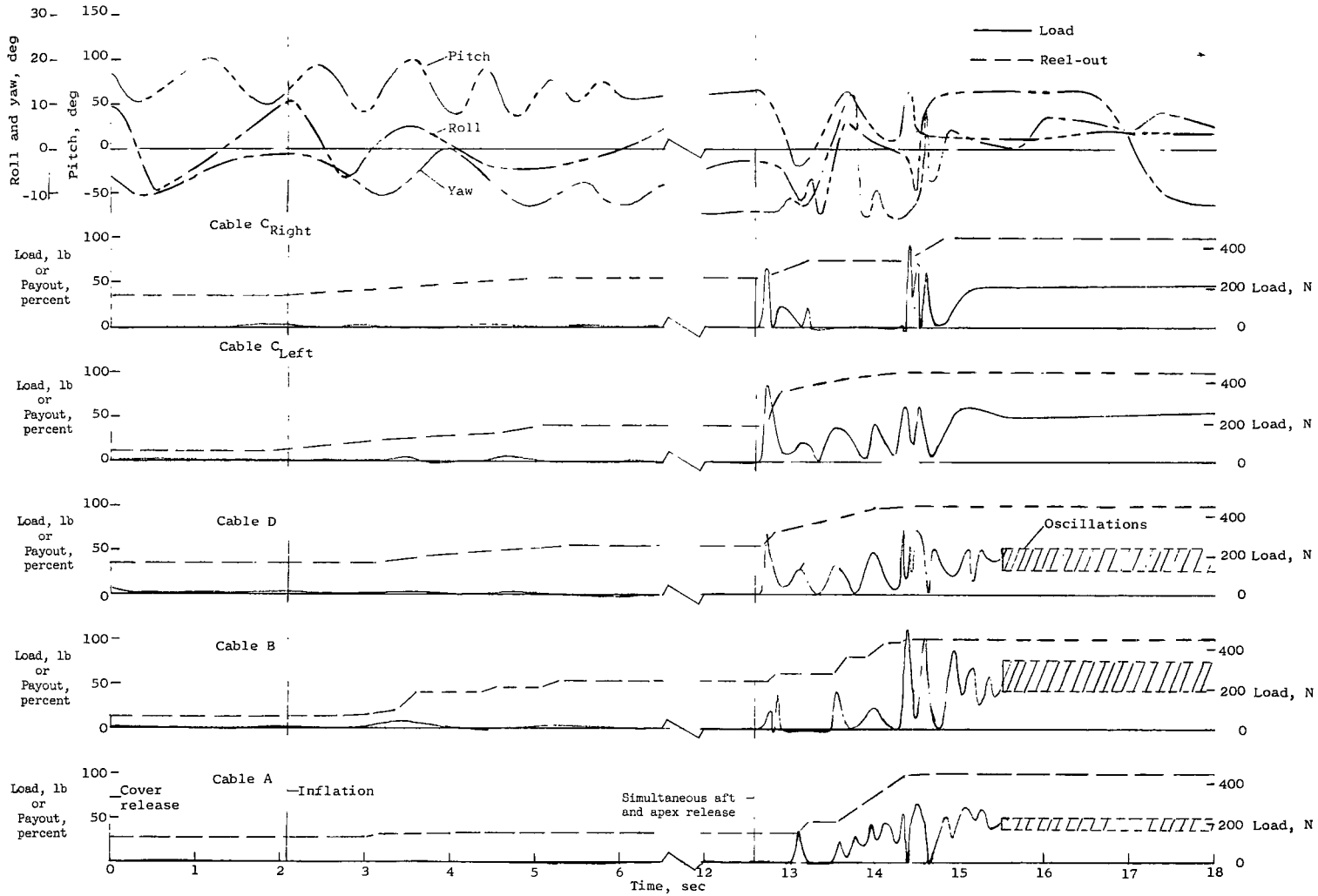

Figure 15.- Time history of sixth deployment in Langley transonic dynamics tunnel. $q = 10.5\ lb/ft^2$ $(503\ N/m^2)$.

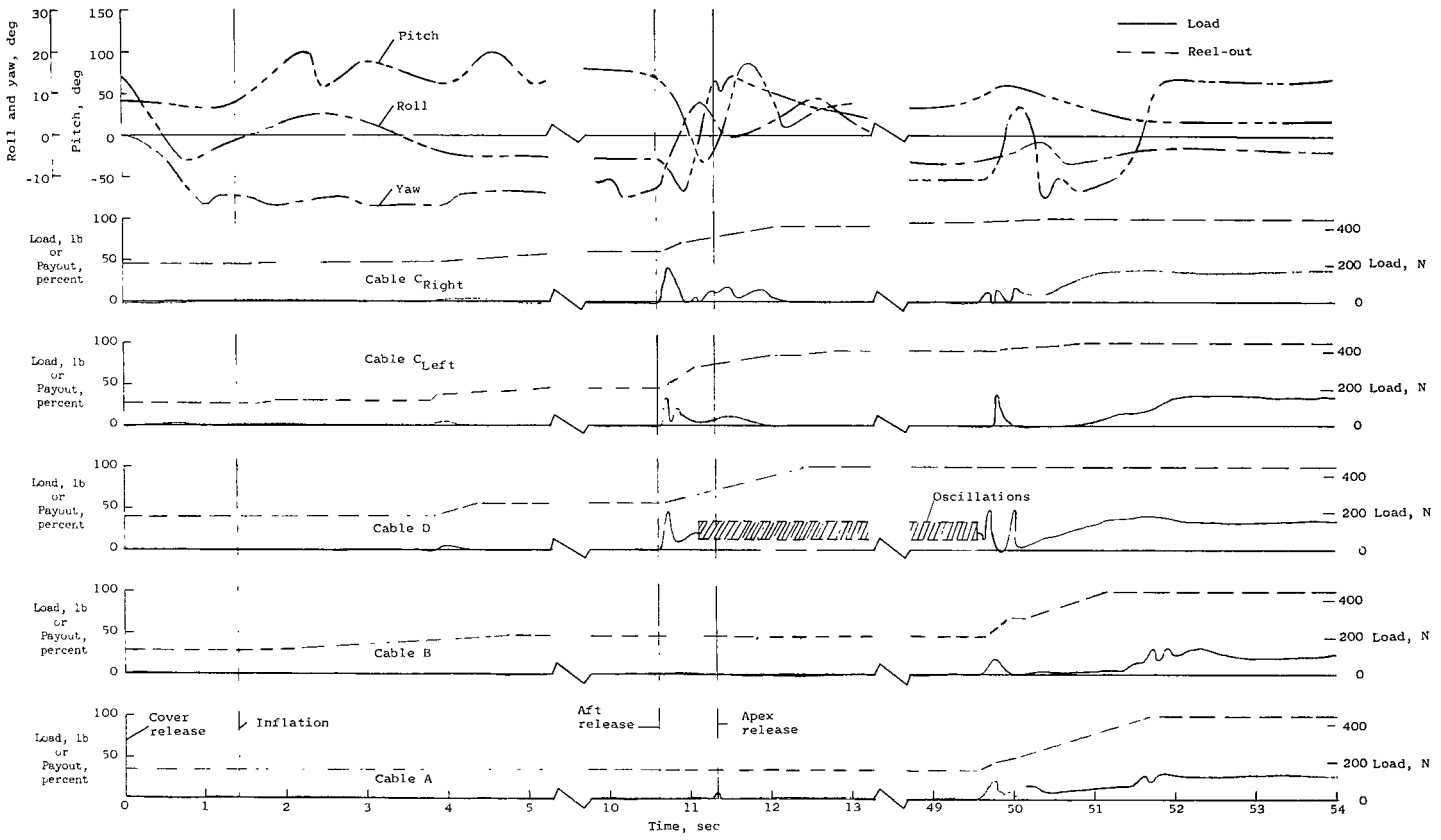

Figure 16.- Time history of seventh deployment in Langley transonic dynamics tunnel. $q = 7.0$ lb/ft^2 (335 N/m^2); model inverted.

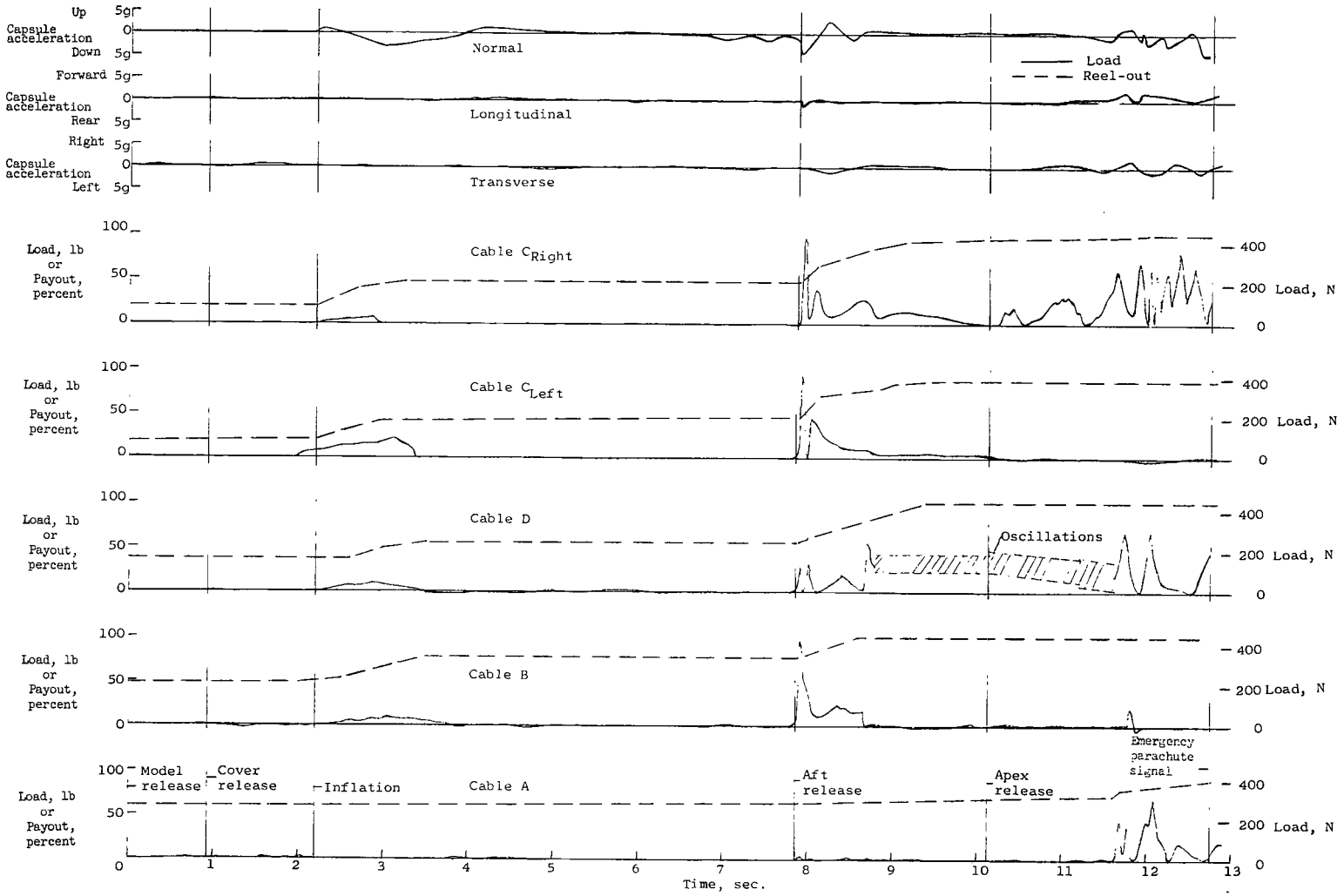

Figure 17.- Time history of first free-flight deployment.

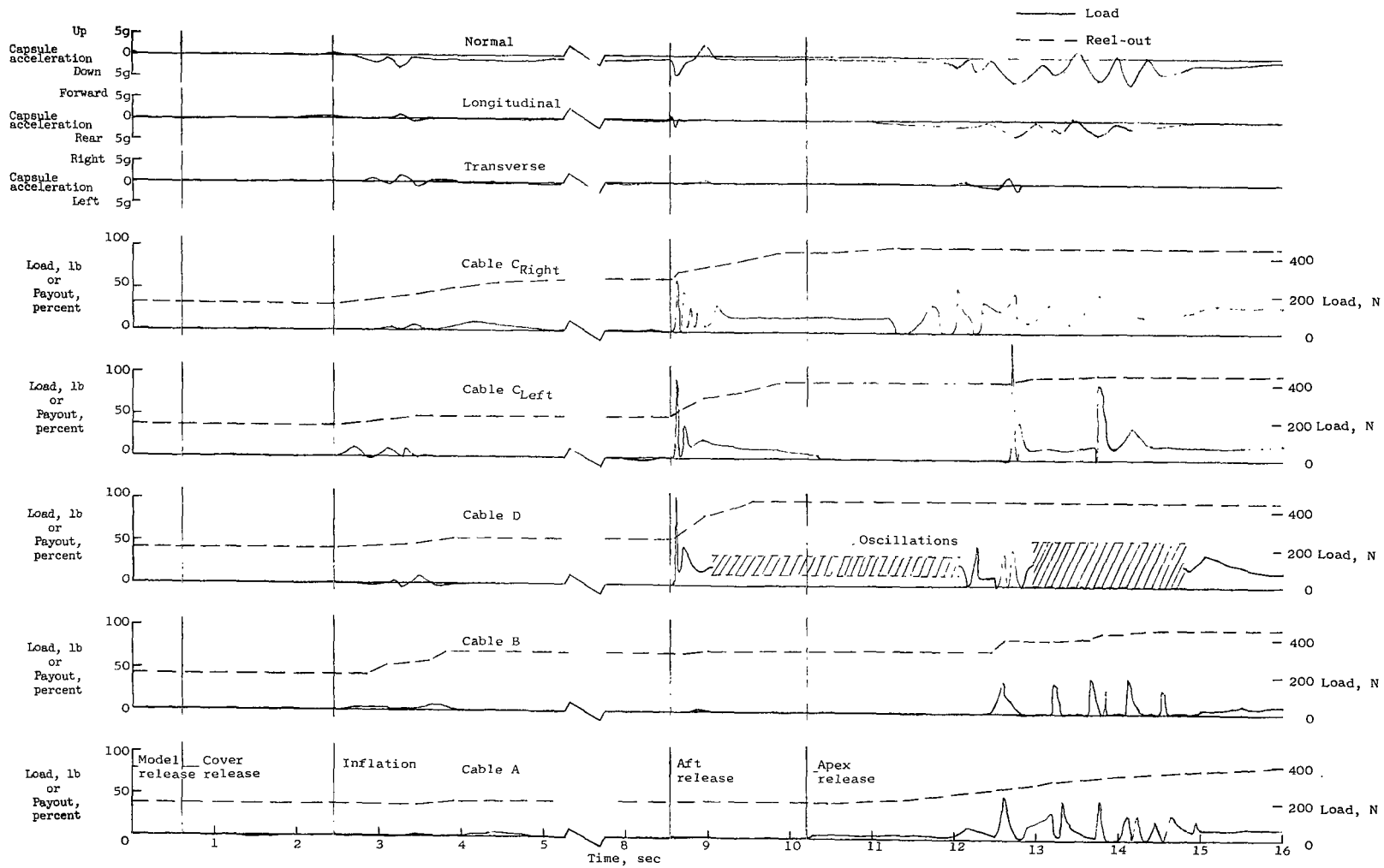

Figure 18.- Time history of second free-flight deployment.

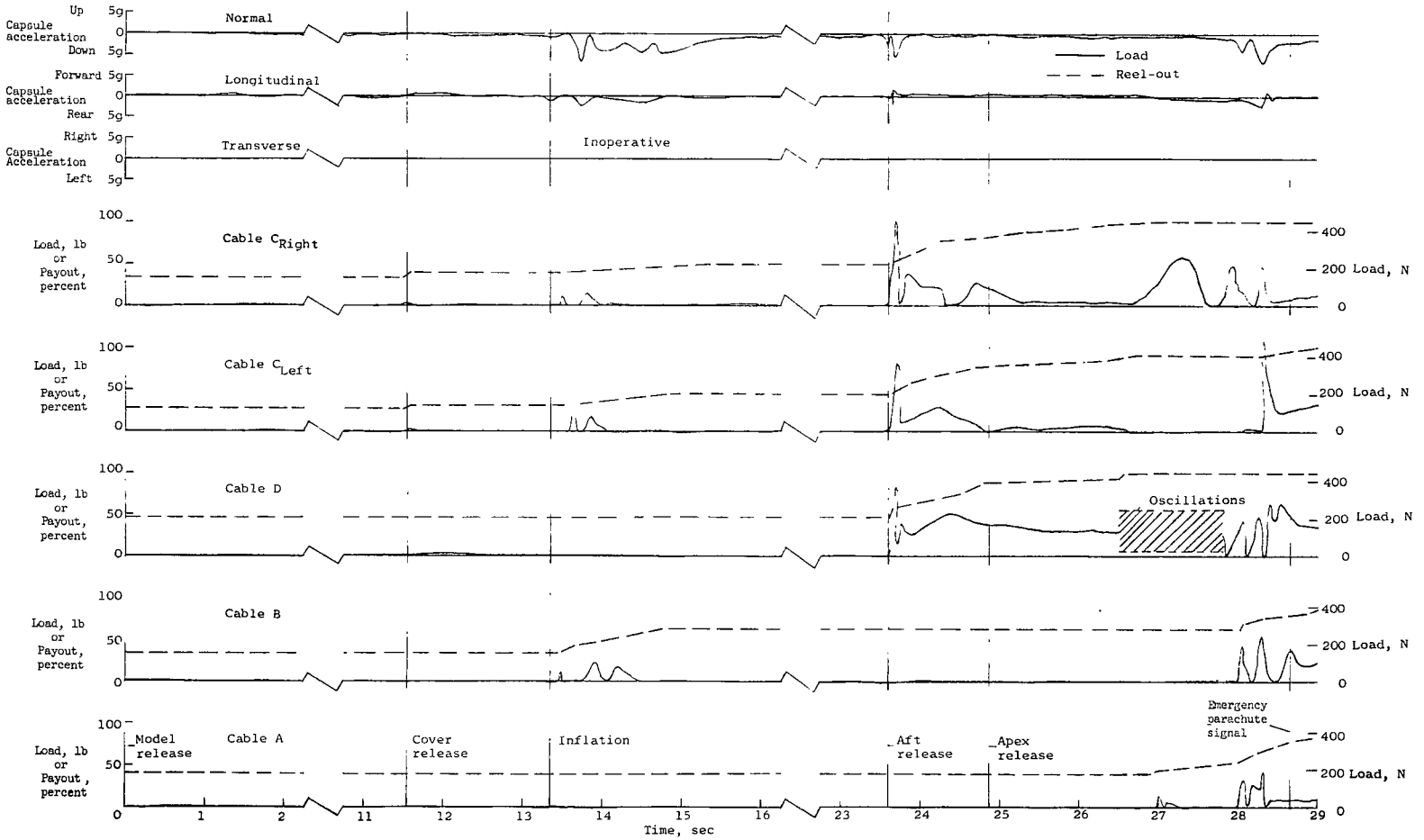

Figure 19.- Time history of third free-flight deployment.

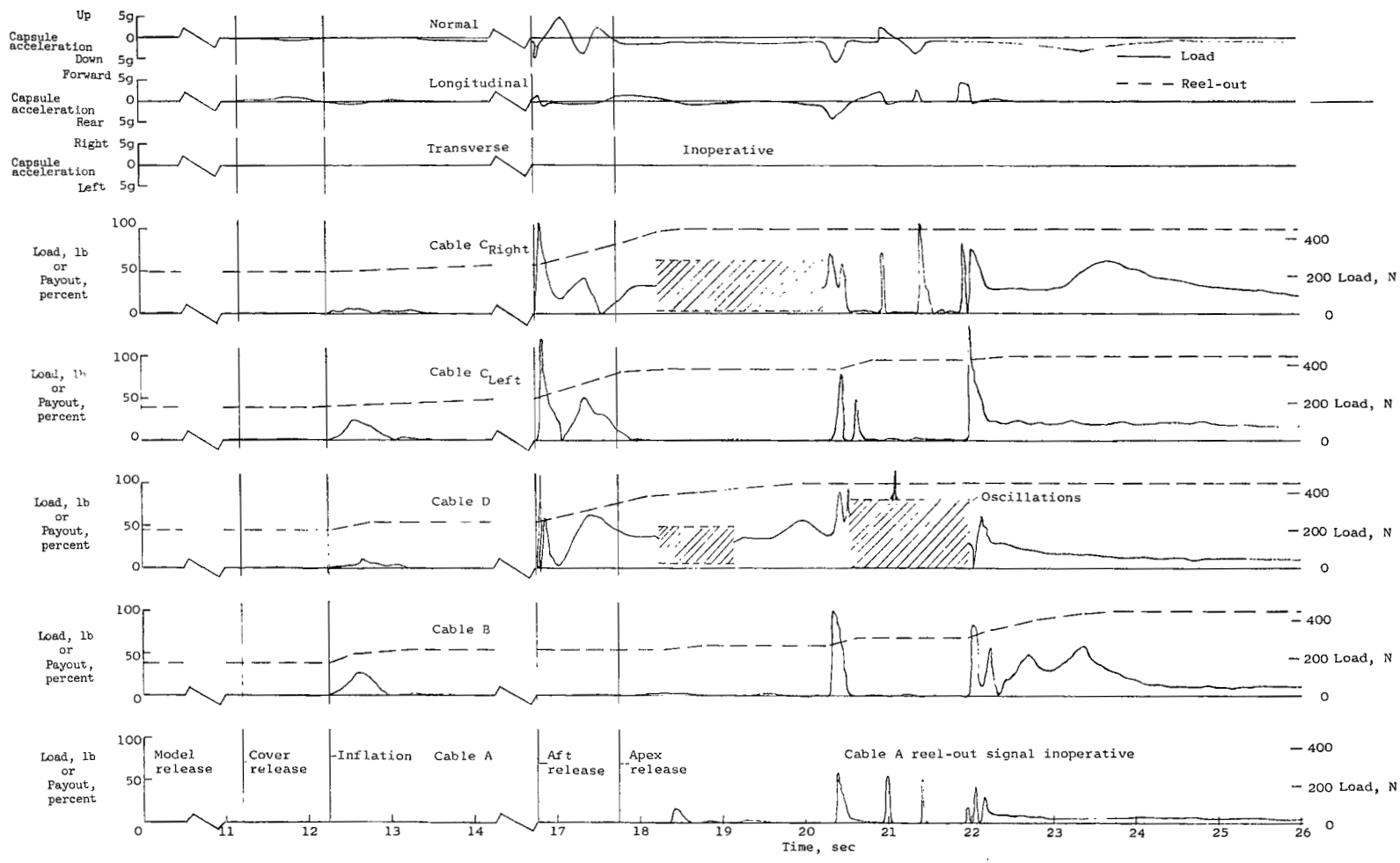

Figure 20.- Time history of fourth free-flight deployment.

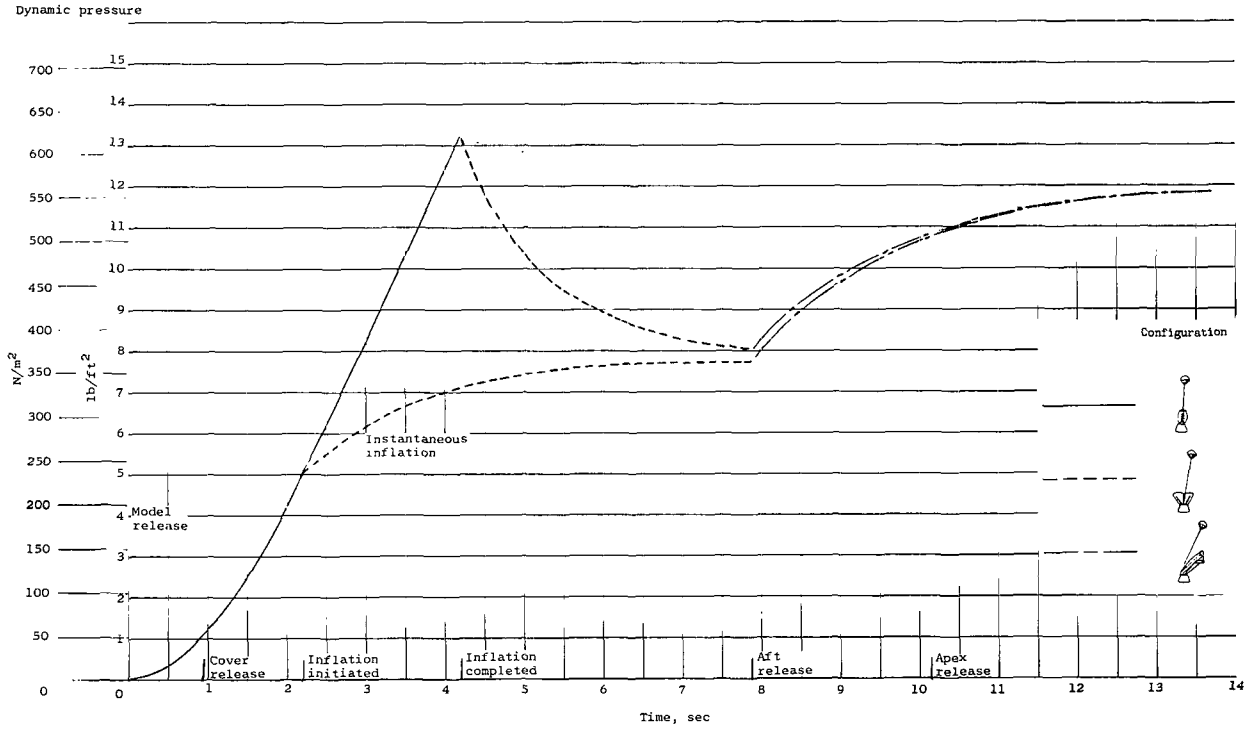

Figure 21.- Calculated dynamic pressure profile of first free-flight deployment.

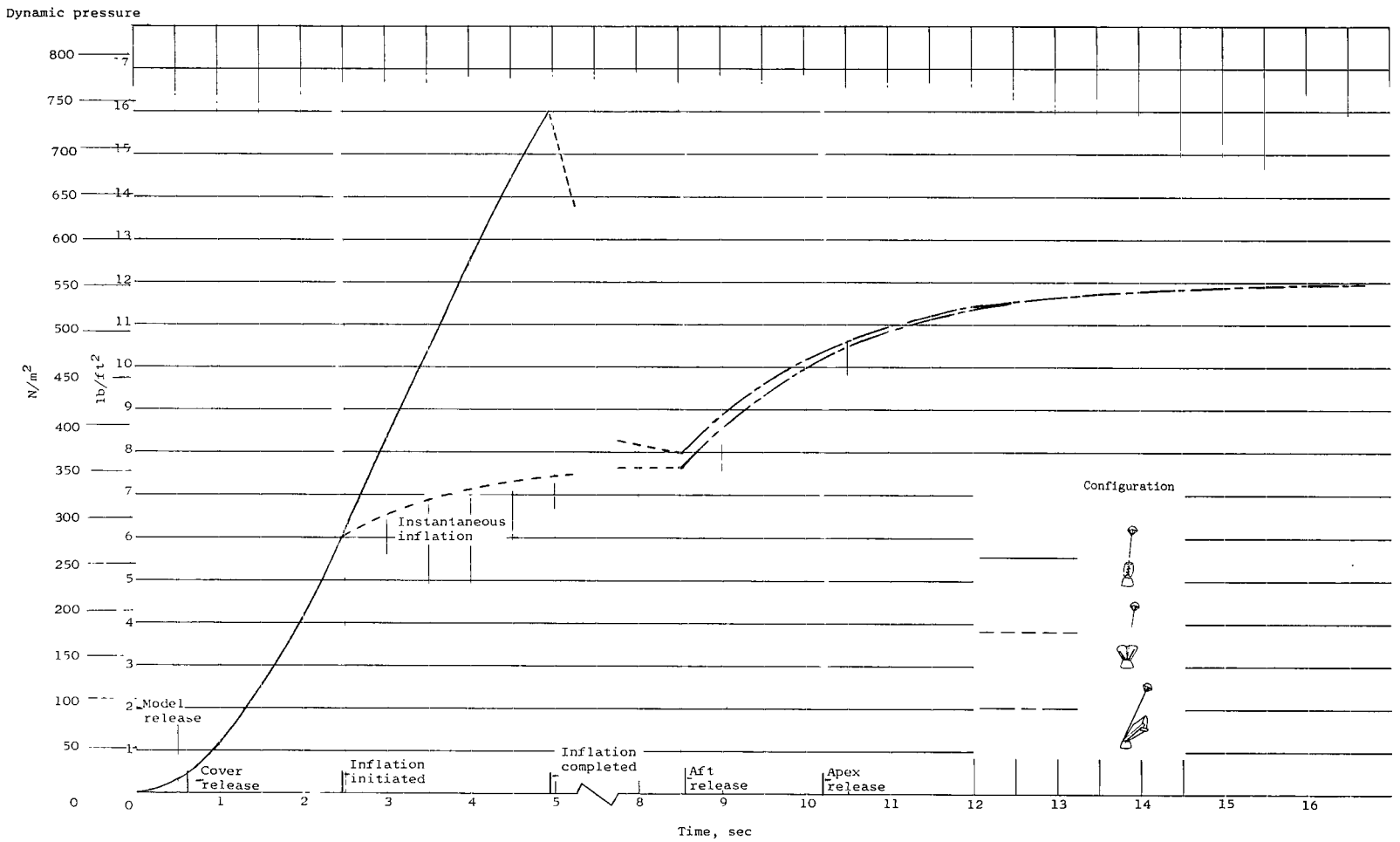

Figure 22.- Calculated dynamic pressure profile of second free-flight deployment.

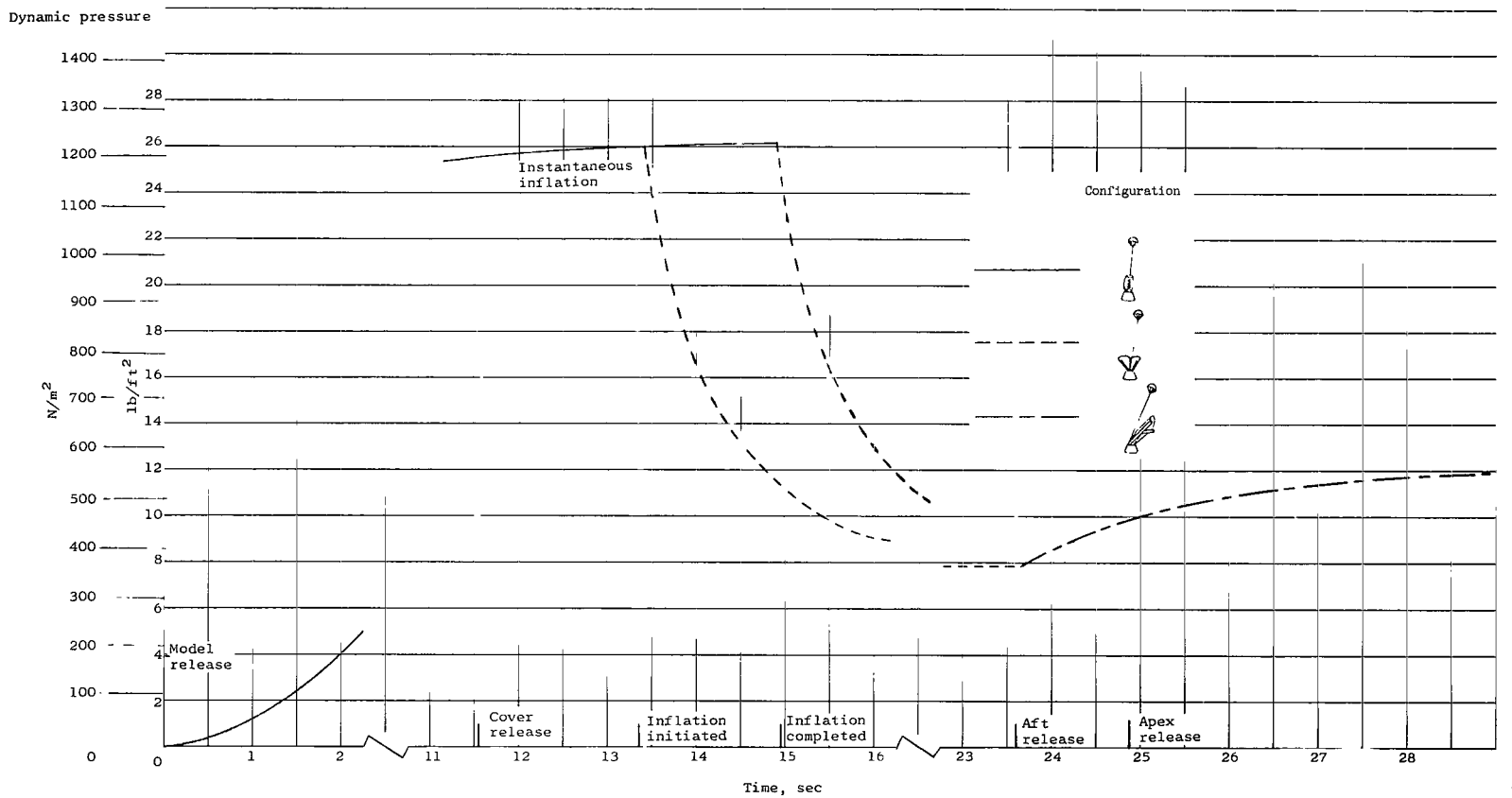

Figure 23.- Calculated dynamic pressure profile of third free-flight deployment.

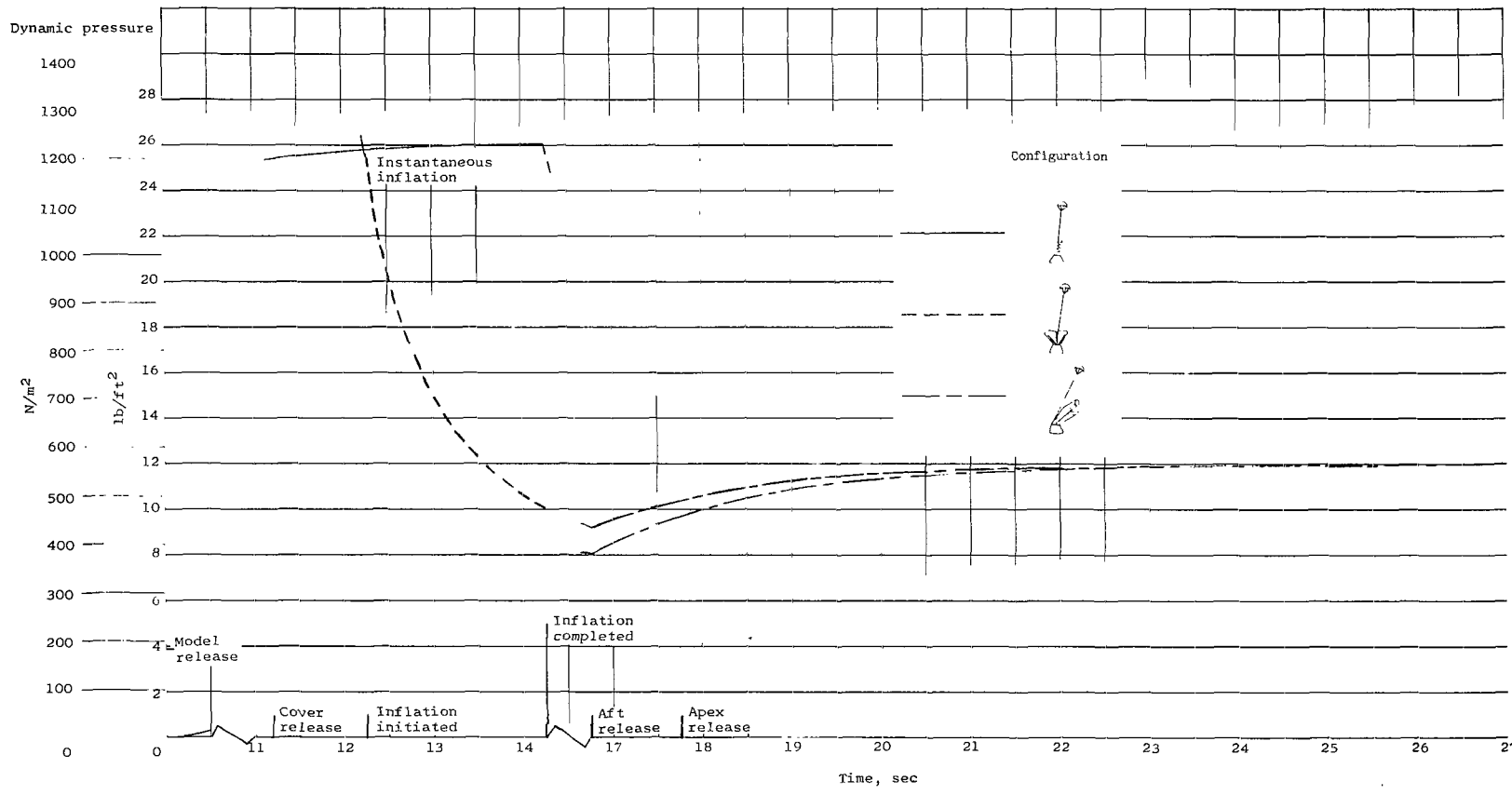

Figure 24.- Calculated dynamic pressure profile of fourth free-flight deployment.

NATIONAL AERONAUTICS AND SPACE ADMINISTRATION
WASHINGTON, D.C. 20546

OFFICIAL BUSINESS

FIRST CLASS MAIL

POSTAGE AND FEES PAID
NATIONAL AERONAUTICS AN
SPACE ADMINISTRATION

"The aeronautical and space activities of the United States shall be conducted so as to contribute . . . to the expansion of human knowledge of phenomena in the atmosphere and space. The Administration shall provide for the widest practicable and appropriate dissemination of information concerning its activities and the results thereof."

—NATIONAL AERONAUTICS AND SPACE ACT OF 1958

NASA SCIENTIFIC AND TECHNICAL PUBLICATIONS

TECHNICAL REPORTS: Scientific and technical information considered important, complete, and a lasting contribution to existing knowledge.

TECHNICAL NOTES: Information less broad in scope but nevertheless of importance as a contribution to existing knowledge.

TECHNICAL MEMORANDUMS: Information receiving limited distribution because of preliminary data, security classification, or other reasons.

CONTRACTOR REPORTS: Scientific and technical information generated under a NASA contract or grant and considered an important contribution to existing knowledge.

TECHNICAL TRANSLATIONS: Information published in a foreign language considered to merit NASA distribution in English.

SPECIAL PUBLICATIONS: Information derived from or of value to NASA activities. Publications include conference proceedings, monographs, data compilations, handbooks, sourcebooks, and special bibliographies.

TECHNOLOGY UTILIZATION PUBLICATIONS: Information on technology used by NASA that may be of particular interest in commercial and other non-aerospace applications. Publications include Tech Briefs, Technology Utilization Reports and Notes, and Technology Surveys.

Details on the availability of these publications may be obtained from:

SCIENTIFIC AND TECHNICAL INFORMATION DIVISION

NATIONAL AERONAUTICS AND SPACE ADMINISTRATION

Washington, D.C. 20546